nature protocols

Consensus statement

https://doi.org/10.1038/s41596-024-00998-w

OBSERVE: guidelines for the refinement of rodent cancer models

Received: 28 February 2023

Accepted: 23 February 2024

Published online: 11 July 2024

Check for updates

A list of authors and their affiliations appears at the end of the paper

Existing guidelines on the preparation (Planning Research and Experimental Procedures on Animals: Recommendations for Excellence (PREPARE)) and reporting (Animal Research: Reporting of In Vivo Experiments (ARRIVE)) of animal experiments do not provide a clear and standardized approach for refinement during in vivo cancer studies, resulting in the publication of generic methodological sections that poorly reflect the attempts made at accurately monitoring different pathologies. Compliance with the 3Rs guidelines has mainly focused on reduction and replacement; however, refinement has been harder to implement. The Oncology Best-practices: Signs, Endpoints and Refinements for in Vivo Experiments (OBSERVE) guidelines are the result of a European initiative supported by EurOPDX and INFRAFRONTIER, and aim to facilitate the refinement of studies using in vivo cancer models by offering robust and practical recommendations on approaches to research scientists and animal care staff. We listed cancer-specific clinical signs as a reference point and from there developed sets of guidelines for a wide variety of rodent models, including genetically engineered models and patient derived xenografts. In this Consensus Statement, we systematically and comprehensively address refinement and monitoring approaches during the design and execution of murine cancer studies. We elaborate on the appropriate preparation of tumor-initiating biologicals and the refinement of tumor-implantation methods. We describe the clinical signs to monitor associated with tumor growth, the appropriate follow-up of animals tailored to varying clinical signs and humane endpoints, and an overview of severity assessment in relation to clinical signs, implantation method and tumor characteristics. The guidelines provide oncology researchers clear and robust guidance for the refinement of in vivo cancer models.

The term cancer comprises a heterogeneous group of complex pathologies that clinically present with different tumor (sub)types, stages and metastatic niches. Many cancers display diverse mechanisms of resistance, either intrinsically developed or acquired under therapeutic pressure. Fostered by emerging technologies, a substantial expansion of available treatment modalities contributed to a paradigm shift from one-size-fits-all toward precision oncology[1–4]. Taken together, this highlights the need for a diverse and well-characterized toolbox of preclinical models in the cancer research area. To reliably recapitulate a cancer patient, accurately study tumor biology and test the efficacy and safety of anticancer agents, a variety of in vitro and in vivo model systems have been generated.

Despite the availability of many nonanimal methods and ongoing efforts to further develop animal-free alternatives, the need for complex and heterogeneous animal models recapitulating various aspects of the disease of interest persists. This is clearly observed in the steady number of laboratory animals used across basic, translational and applied research worldwide and in the European Union (EU)[5]. Approximately 1 million mice were utilized in the EU in oncology research in 2019, representing one of the top four disciplines for

e-mail: stephanie.devleeschauwer@kuleuven.be

animals used across basic and translational research applications (EU 2019 report[5]). Indeed, preclinical models are integral to the development of new treatment options[3,6–8], investigating systemic metastasis[9], exploring side effects or resistance upon demanding treatment regimens[10,11] and studying the interplay between the tumor and its micro-environment[12,13].

Reproducibility and replicability of experiments and results are often challenging in biomedical research[14–17]. As recently demonstrated by a large reproducibility study in preclinical cancer biology, only 46% of published results could be successfully reproduced[18]. Indeed, several 'natural' inescapable hurdles contribute to the limited reproducibility of preclinical findings including innate biological heterogeneity as well as the use of nonstandardized methods or materials. Moreover, poor study design, insufficient statistical power and lack of adherence to reporting standards contribute to bias and poor reproducibility. To maximize the likelihood of successful clinical translation, preclinical biomedical studies require stringent design. This should include appropriate research planning and proper study design, standardization of methods, protocols and disease models, and thorough and transparent reporting. Previous efforts to increase reproducibility have been made via the Planning Research and Experimental Procedures on Animals: Recommendations for Excellence (PREPARE) and Animal Research: Reporting of In Vivo Experiments (ARRIVE) guidelines. The PREPARE guidelines provide guidance on how to plan animal experiments that are reproducible and scientifically robust. In addition, PREPARE addresses animal welfare issues and provides resources for additional guidance on more specific topics[19]. The ARRIVE guidelines aim to improve the reporting of animal research by providing a checklist of information to include in publications describing in vivo experiments[20,21]. Thus, whereas the PREPARE guidelines[19] provide guidance on how to plan animal experiments, the ARRIVE guidelines mainly focus on the proper reporting of animal experiments[20,21]. Despite the many topics covered in both comprehensive checklists, clear and standardized guidelines on the monitoring of animals during the experiment are rather scarce.

As highlighted in the EU Parliament in 2022, there is a tendency of the EU and its Member States to focus on reduction and replacement, whereas the third R, refinement, is under considered and lagging behind[22]. The 3Rs concept as originally described by Russell and Burch defined refinement as 'any decrease in the incidence or severity of inhumane procedures applied to those animals which still have to be used'[23]. In addition, the 3Rs state that the 'object of refinement is simply to reduce to an absolute minimum the amount of distress imposed on those animals that are still used'. In many cases, an additional definition is attributed to refinement as the reduction or elimination of distress and pain. In general, the ethical aim of humane use and care of animals in research is to spare them from all substantial unpleasant experiences not necessary for the purpose of research and to enhance animal well-being[24].

With the inherent use of a large number of animals and a variety of animal models in oncology, there are numerous opportunities for refinement. Nevertheless, it is remarkable that practical guidelines on this topic are rather sparse. Publications remain either very general, providing only specific guidelines for the subcutaneous (SC) models[25–27] or are highly specific for one particular model[28–35]. Therefore, in line with IMPROVE[36]— a guideline for in vivo ischemic models—the Oncology Best-practices: Signs, Endpoints and Refinements for in Vivo Experiments (OBSERVE) guidelines aim to bridge this gap, offering a comprehensive set of practical and specific recommendations on refinement in murine cancer models for scientists, veterinarians and animal care staff.

In addition to mice and rats, several other mammalian models are used in cancer research such as pigs, dogs and nonhuman primates, in addition to some nonmammalian models including drosophila and zebrafish[2,37–41]. The spontaneous canine, feline and nonhuman primate tumor models[41–44] provide a unique platform for evaluating novel therapeutic regimens in the context of an intact immune system. Other, nonspontaneous models, however, require genetic modification[45–49]. Similar to murine models, genetic manipulation and transgenesis (e.g., clustered regularly interspaced short palindromic repeats (CRISPR)) is applied to generate severe combined immune-deficient animals for xenotransplantation studies[50] or models that are capable of developing tumors in various organs[51–54]. Although some of the clinical signs in patients associated with a specific tumor type may be similar in other mammals, refinement during implantation, induction and importantly during tumor development may differ notably between species. Therefore, these guidelines focus on murine models and do not include other species, as broadening to other species would be beyond the expertise of the authors and European consortia involved in drafting the OBSERVE guidelines.

Commonly used murine model systems include patient-derived xenografts (PDX), cell line- or organoid-based xenografts, humanized mice and autochthonous models such as spontaneous, chemically induced or genetically engineered models (GEM) (Fig. 1). Whereas syngeneic cells can be transplanted into fully immunocompetent mice, xenogeneic human cells and allogeneic mouse cells must be transplanted into immunocompromised mice to avoid rejection by the host. Indeed, immune-deficient animals are more vulnerable to a variety of pathogens and opportunists and are thus best housed and manipulated in a specific pathogen-free environment. Immune competence therefore directly impacts and has practical consequences on design, preparation and execution of animal experiments.

Irrespective of the immune status and the route of tumor induction, whether spontaneous or via orthotopic transplantation, the main signs of disease and adverse effects due to tumor development are likely to manifest in a similar manner. For example, ascites can be expected to develop in ovarian cancer models, whether human tumor fragments are implanted orthotopically[55], murine cells are injected intraperitoneally or tumor development occurs spontaneously in GEMs[56,57]. In contrast, SC implanted tumors will generate a different but very specific set of clinical signs driven by replication rate, invasiveness, tendency to ulcerate and site of inoculation. Although in general the set of clinical signs will be similar in SC models regardless of the tumor type, aggressiveness directly linked to tumor (sub)type will also have an impact. Likewise, therapeutics such as cisplatin will exhibit similar side effects in treatment studies of different tumor types[10].

In a stepwise approach, the OBSERVE guidelines aim to address multiple aspects of an in vivo cancer study. First, we address appropriate preparation and refinement of specific implantation methods. Then, we describe the clinical signs which may be associated with a specific tumor type and how these signs can be assessed. Finally, we focus on refinement during tumor growth using a two-pronged approach: how to monitor tumor growth (Box 1) on the one hand and how to follow-up on the animal on the other hand (for example when dealing with loss of appetite and consequent body weight (BW) loss; Fig. 2). The latter is done by providing a comprehensive and specific set of monitoring sheets for different clinical signs including the description of specific humane endpoints (HEPs). HEPs are specific timepoints at which measures to alleviate pain and distress are taken, and ultimately offer criteria for humanely killing of the animals. HEPs must be tailored to the objective of the study and aim to reduce overall severity. Therefore, to facilitate definition and use of HEPs, we have developed generic and specific monitoring sheets that stratify HEPs into 'actions to be taken' and 'criteria for humane killing'. A clear overview of severity assessment in relation to clinical signs, implantation method and tumor specificities is provided. Of note, HEPs and prospective severity assessment of an experimental protocol must be defined upfront, and thus guide decision-making policy of an animal study.

https://doi.org/10.1038/s41596-024-00998-w

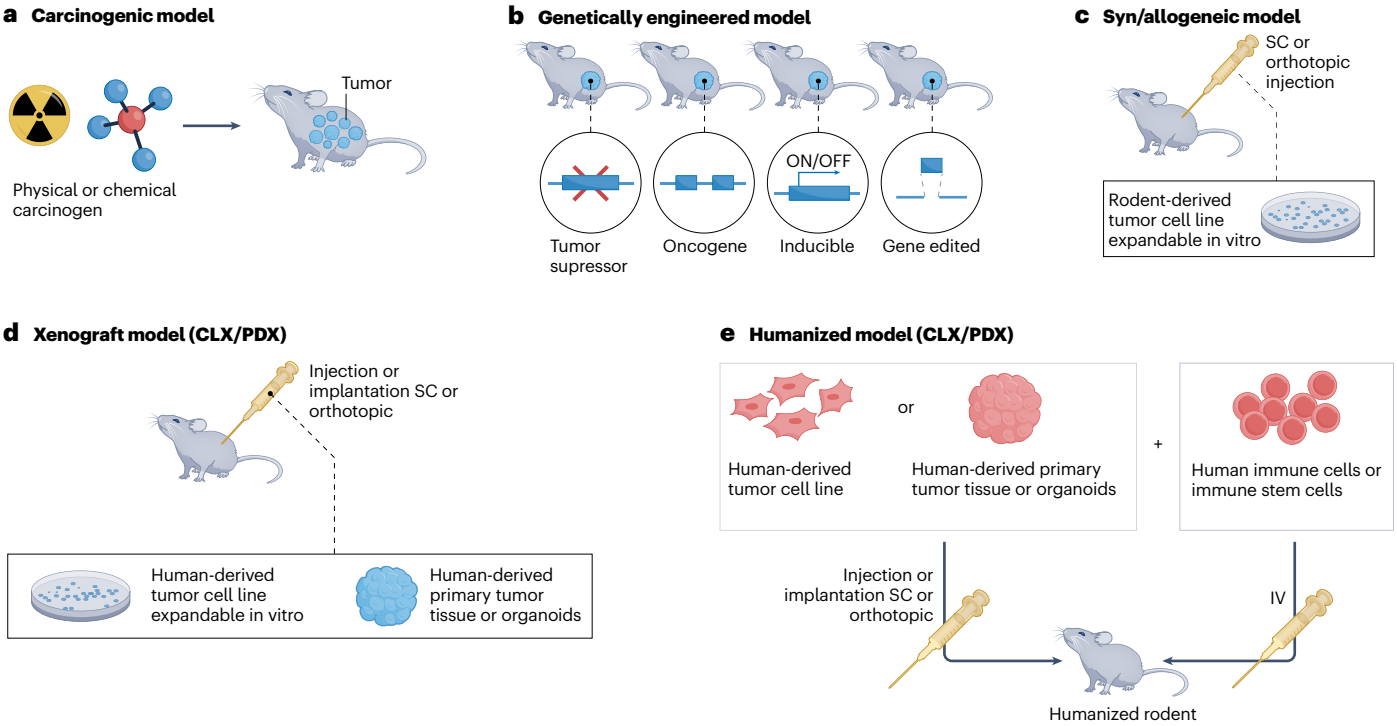

Fig. 1 | Schematic overview of types of rodent tumor model. a, A carcinogenic model: cancer model established in immunocompetent animals by applying a physical and/or chemical carcinogen(s) inducing genetic alterations causing tumor growth. **b**, A genetically engineered model: cancer model based on the genetic alteration of oncogenes or tumor suppressor genes or administration of exogenous activating agents for organ-specific tumor development. **c**, A syngeneic model and allogeneic model: engraftment of mouse or rat tumor cells or organoids in, respectively, a genetically identical, immune competent strain or a genetically different, immune deficient strain of the same species. Cell lines can be generated from a chemically induced or genetically engineered model. **d**, A xenograft model: xenograft in immune deficient animals of a cell line, a tissue piece or organoids generated from a cancer biopsy, usually from human origin. **e**, A humanized model: xenograft model in immunodeficient mice previously engrafted with human immune cells. CLX, cell line xenograft; PDX, patient-derived xenograft.

Method

The OBSERVE guidelines were developed by an expert group of laboratory animal veterinarians, animal welfare officers and researchers involved in preclinical research with an interest in murine cancer studies. The generation of the OBSERVE guidelines was supported by a steering committee, a larger expert panel and two consortia in animal research, EurOPDX (www.europdx.eu) and INFRAFRONTIER (www.infrafrontier.eu). EurOPDX, the European consortium on PDX models, is actively developing standard operating procedures for quality control and in vivo drug efficacy studies, thereby fostering reproducibility and replicability in preclinical research. INFRAFRONTIER, the European Research Infrastructure for the generation, phenotyping, archiving and distribution of model mammalian genomes, largely addresses the issue of reproducibility and replicability by developing internal quality principles[58] for its different service areas. As such, they provide a quality framework for its operational activities.

The steering committee established four key objectives for the guidelines:

1. Comprehensible for a diverse audience, including animal caretakers and researchers with minimal experience in animal studies.
2. Practical and precise with specific guidelines per tumor type or site of growth, including suggested endpoints, using tables and monitoring sheets
3. Focus on refinement and reproducibility, avoiding housing and husbandry, description of specific cancer models, cell types, etc.
4. Applicable to a wide-range of tumor models

The steering committee's initial draft was based on the committee members' experience and literature focused on refinement and reproducibility. The guidelines were further refined with the addition of experts in specific areas of needs. In parallel, draft guidelines were reviewed by EurOPDX and INFRAFRONTIER.

The OBSERVE guidelines are designed to guide researchers in a step-by-step approach. First, the researcher is encouraged to refine the animal study by proper preparation and optimizing the method of implantation. Then, we list which clinical signs and/or adverse effects may be expected in a specific tumor model (Table 1). Next we explain these clinical signs in more detail: their etiology, recognition and monitoring (Table 2). This is followed by selecting the most appropriate method to follow-up tumor growth (Table 3) combined with comprehensive monitoring sheets (Tables 4–12) specifically for each model. The latter include clear actions to be taken as well as the description of discrete HEPs. Finally, a severity classification (Table 13) is given for the different cancer models.

Refinement during implantation or induction of tumors

The following points should be considered when selecting an appropriate animal model: for previously established models, consult existing literature and experienced colleagues to better comprehend the model. Factors to be considered include tumor growth pattern, likelihood of metastasis and development of paraneoplastic syndromes such as cachexia. If a novel model is to be generated, pilot studies should be conducted to analyze the model-specific features before using a larger cohort of animals.

When transplanting tumors into animals, precautions should be taken to ensure long-lasting engraftment, avoid host-versus-graft reaction and prevent the development of infectious disease of the host. These considerations include (a) careful selection of the correct mouse strain (genetic background and immune status) and suitable

https://doi.org/10.1038/s41596-024-00998-w

BOX 1

Tumor measurement with a caliper

The length of the tumor is intended as its longest axis; the width as its shortest axis; and the depth is usually not used in the calculation (because it is hard to measure accurately), instead it is preferred to use the smallest measurement (i.e., width) twice. The following formulas may be used to measure tumor volume:

1. **Ellipsoid variants**
   $4/3\pi r_1 r_2^2$
   where r_1 is the longest radius and r_2 is the shortest radius assuming width and depth of the tumor are equal or,
   $4/3\pi r_1 r_2 r_3$
   where r_1 is the longest radius and r_2 and r_3 are the shortest radius (width and depth) or,
   $(\pi a b^2)/6$
   where a is the longest axis and b is the shortest axis, assuming width and depth of the tumor are equal or,
   $(\pi abc)/6$
   where a is the longest axis, and b and c are the short axes.
2. **Modified ellipsoid**
   $(ab^2)/2$
   where a is the longest axis and b is the shortest axis, assuming width and depth of the tumor are equal.

Image **a** of the figure shows the axes and radiuses of a SC tumor, which are used to measure tumor volume; the correct placement of the caliper is shown in **b**; and an incorrect placement of the caliper is shown in **c**. Correct placement of the caliper is of extreme importance for the correct measurement of tumor volume. As a rule of thumb: it should always be possible to move the caliper over the tumor when measuring the length/height. As such, the tumor is not 'squeezed' and its volume not underestimated (notice the difference in volume measurement between **b** and **c**). To avoid observer bias, a blind study design should be set up especially in treatment studies.

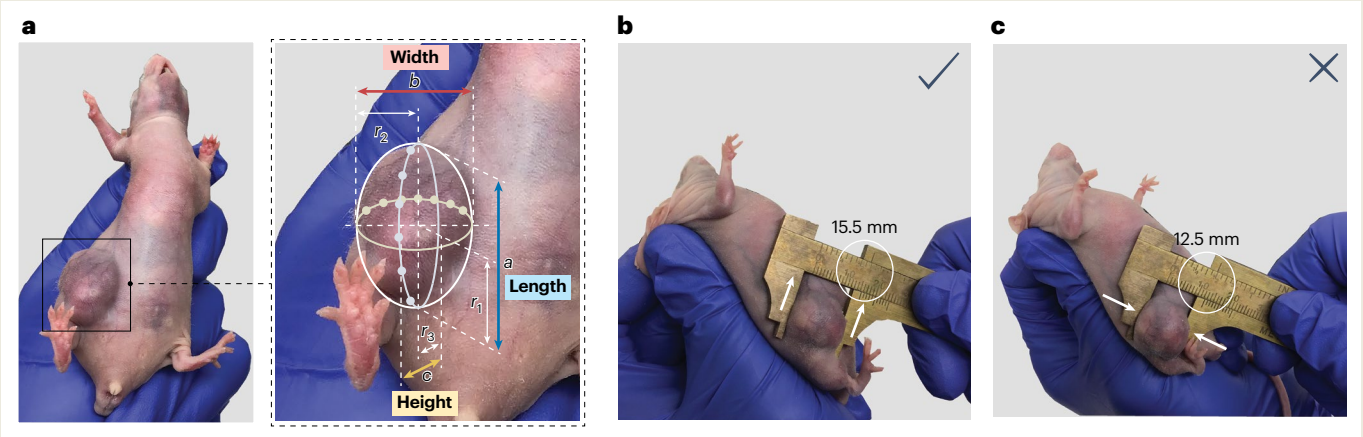

tumor characteristics, (b) PDX tumor transplants should be actively dividing cells derived from a nonulcerated, nonhemorrhagic and nonnecrotic tumor[59], (c) cell lines should be viable and proliferating and less than 80% confluent prior engraftment, (d) it must be ensured that cells are not contaminated with mycoplasma or other pathogens as this may compromise experimental results or cause disease outbreaks among laboratory animals. Therefore, screening of tumors for rodent and human pathogens (in case of PDX) is strongly recommended[60–63].

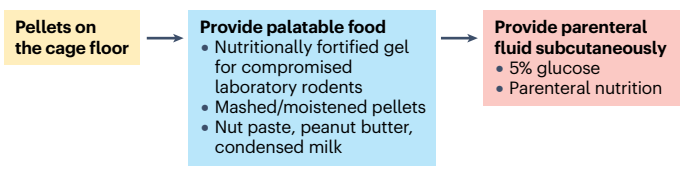

Fig. 2 | A stepwise approach for providing extra water and nutrition to rodents. When rodents are anorexic, providing easy to reach food and/or appetent food might stimulate their appetite. When BW loss is expected, providing appetent food early on allows to overcome the classical neophobic response. In case of not eating or dehydration, parenteral fluids should be given. Considering variation in food may influence your outcome, control animals should receive the same feeding regimen.

Tumor implantation should be performed by appropriately trained staff using aseptic techniques and peri-operative care must include the appropriate administration of anesthetic and analgesic regimens (Box 2). The size of incisions (when required) should be minimized to reduce postprocedure pain and appropriate needle sizes and injection volumes should be utilized[64,65]. Tumor transplantations should be performed expeditiously following donor tissue collection. Co-injection of a dye to ensure correct tumor localization may help in training of injectable transplantation techniques[66,67]. The use of a separate set of surgical instruments for the manipulation of tumor tissue—distinct from instrumentation used to manipulate nontumor tissue—is strongly recommended to prevent the spread of tumor cells by surgical instruments.

Note that orthotopic growth better models the human condition as compared with SC implantation, as demonstrated in breast cancer[68–70]. In addition, orthotopic implantation seems to achieve better engraftment rates compared with SC engraftment[71].

General as well as specific recommendations for tumor implantation are provided.

SC tumor transplantation. SC tumors should be implanted on the dorsum or flank. These sites are less likely to result in site-related morbidity or interfere with normal body functions (locomotion, breathing, etc.).

https://doi.org/10.1038/s41596-024-00998-w

Table 1 | Clinical signs associated with organ-/system-specific tumor development

	General signs				Specific signs									Refs.
	Anorexia and BW loss[a]	Altered appearance and behavior	Pain: demonstrated	Pain: assumed	Icterus	Respiratory signs	Ascites	Anemia	GI signs	Neurological signs	Locomotor signs	Urinary signs	Cutaneous ulceration	
GI tract														
Oral cavity	x	x	x											128–131
Esophagus	x	x		x										132,133
Gastric	x	x		x	x		x	x	x					134–137
Pancreas	x	x	x		x		x							34,130, 131,138,139
Colorectal	x	x	x					x	x					33,140–142
Liver + gallbladder	x	x		x	x		x							143–146
Urogenital system														
Kidney (+ adrenal)	x	x		x								x		147
Bladder	x	x	x									x		148–152
Prostate	x	x		x								x		153–156
Uterus	x	x		x			x	x				x		157
Ovary	x	x		x			x					x		55,158,159
Cervix	x	x		x								X		160–162
Mammary	(x)	x	x								x		x	131
Nervous system														
Brain tumors	x	x		x						x				79,163,164
Other CNS	x		x							x	x			130,131,165
Peripheral nerve	x	x	x				x	x		x	x			166
Soft tissue and bone														
Soft tissue	Clinical signs of soft tissue tumors depend on the location, please refer to other organs to have an indication of adverse effects													
Bone (+ multiple myeloma bone disease)	x	x	x								x			130,131, 167,168
Respiratory tract														
Upper respiratory tract: nose, nasal cavity, paranasal sinuses	x	x	x			x				x				169,170
Lung	x	x	x			x								171–173
Hematopoetic and lymphoid														
Lymphoma and myeloma	Signs of lymphoma/myeloma depend on the location, please refer to other organs to have an indication of adverse effects													
Leukemia	x	x		x		x	x	x	x	x				29,174
Endocrine														
Pituitary	x	x		x						x				175,176
Thyroid	x	x		x		x								177
Skin														
	(x)	(x)											x	178
SC tumors														
	(x)	(x)											x	25,179
Miscellaneous														
Eye			x											
GVHD in humanized mice[b]	x	x						x	x					180,181

[a]Note that some models may also cause an increase in BW due to ascites, tumor mass, for example. [b]Although strictly not a tumor type, humanized mice are often used in cancer research and GVHD is accompanied by a series of typical signs.

Table 2 | Clinical signs associated with cancer models: description, recognition and etiology

Clinical sign	Description	How to assess?	Etiology
General signs			
Anemia	Reduced number of red blood cells and/or low hemoglobin	Evaluate the color of the mucous membranes (around the eyes, mouth and tongue) and skin (interdigital spaces), which should be pink. If they are pale, anemia is probably present.	Blood loss in cancer is usually due to ulcerating tumors, necrosis or inflammation especially in GI or urogenital tumors. A decreased production of red blood cells may be present in tumors involving the bone marrow (e.g., leukemia, lymphoma or bone marrow metastasis), inflammation present in chronic conditions (such as cancer) or myelosuppressive (chemo/radio)therapy. Anemia may also be seen in GVHD as excessive immune activation leads to hemolysis of erythrocytes by foreign antibodies.
Anorexia	Loss of appetite	Is usually seen as weight loss. Weight loss can be determined by weighing the animals (see Box 4 for more information on weight during tumor studies). In many cancer models, body condition score (BCS) is the preferred monitoring tool[182,183]. The absence or marked reduction of fecal pellets in the cage may also be an indication of anorexia. Food intake can be assessed in a metabolic cage (requires single housing) or by weighing food. In cancer studies this is often not done or even necessary.	Anorexia, accompanied by BW loss and ultimately dehydration (see below), can be an adverse effect of many tumor types but is also a known side-effect of commonly used (chemo) therapeutics such as cisplatin. Weight loss can also result from the release of biologically active substances by the tumor or the host.
Ascites	Fluid accumulation in the abdomen	Seen as abdominal distention that may quickly increase; animal looks potbellied. The distension can usually be depressed in contrast to abdominal distension resulting from a mass or organ enlargement.	Cancer can metastasize to the peritoneum leading to vascular and lymphatic permeability, and subsequently, the accumulation of fluid causing malignant ascites. Tumors can also metastasize to the liver or lymphatic system causing increased pressure, hampering the return of fluid from the abdomen to the heart.
Cachexia	A 'wasting' disorder that results in extreme weight loss, loss of muscle and adipose tissue	Loss of muscle and fat results in skeletal structures being clearly visible, animals have a BCS[182,183] of 1.	Cachexia is a common complication in cancer. It is caused by catabolism factors produced by tumors and physiological factors such as proteolysis and autophagy. Cachexia is characterized by anorexia and metabolic disturbances
Dehydration	Reduction in total body water	Dehydration can be assessed by pinching and gently lifting (tenting) the skin over the shoulder blades (skin turgor test). Normally, the skin will quickly return to its original shape. If the tent remains or is slow to resolve, the animal is dehydrated. In the case of severe dehydration, animals may be weak, immobile and may have sunken eyes[184].	Caused by an imbalance between uptake and loss of fluids. In cancer, this is usually due to anorexia (see above) but can also be a consequence of severe diarrhea (see below).
Icterus	Yellow discoloration of the skin, mucus membranes and eyes, also known as jaundice or hyperbilirubinemia	Yellow pigmentation of the skin, tissues and body fluids; usually observable in the hairless parts of the body. Icterus is easier to see in hairless or albino mice.	Icterus is caused by the accumulation of bilirubin that cannot be metabolized by the liver and secreted in the bile due to cancer of the liver, chemotherapy or obstruction of the bile duct by a tumor.
Pain	An unpleasant sensory and emotional experience associated with, or resembling that associated with, actual or potential tissue damage[185]	As rodents are prey animals, they modulate the display of pain. It is beyond the scope of this paper to provide detail on pain assessment. Pain assessment tools include: the mouse and rat grimace scale[186,187], nest building[188], burrowing[189] and behavioral changes[190–192]. Pain in mice and rats is usually easier to detect when animals are observed undisturbed during the dark (active) phase of the light cycle.	Pain in cancer is caused by pressure of the tumor on nervous tissue, bones or organs. Certain tumor types such as bone, pancreas, and head and neck are known to be painful in rodents and are used to model cancer pain[130,131]. However, as pain is often reported in human patients in many different tumor types, we may assume it is present in many different models, although often not studied or reported in rodent cancer studies. Pain may also be caused by the implantation (surgical or through HDTVI) or the treatment e.g., chemotherapy-induced neuropathy.
Cutaneous ulceration	The loss of epidermis and at least the superficial part of the dermis overlying a growing tumor due to necrosis	The skin overlying the tumor is open, exposing the underlying tissue. Ulcers may be dry and develop a scab or have a wet aspect due to fluid and/or blood loss. Some ulcers have a sunken aspect and look cratered. For pictures of cutaneous ulcerating tumors, see monitoring sheet of cutaneous ulcers (Table 12)	Cutaneous ulceration may be caused by alterations in blood supply to the overlying skin causing necrosis. It may also be caused by rapid growing tumors wherein the skin's ability to stretch is exceeded. Ulceration can also be caused by mechanical or self-induced trauma or experimental therapy leading to death of tumor cells, e.g., by irradiation.
Respiratory signs			
Dyspnea	Labored breathing	Observed as difficult breathing (requiring more effort), abnormal pattern (abdominal heaves or increased chest expansion), open-mouth breathing or increased movement of the nostrils. As dyspnea in cancer models only becomes visible in advanced stages of disease, a stress-test (see monitoring sheet for respiratory signs (Table 6) and Fig. 3)) can aid in determining respiratory problems earlier[172]. Gasping or open-mouth breathing is a sign of advanced dyspnea.	Dyspnea and tachypnea can occur when tumors develop in or near the lungs and airways, by fluid accumulation around the heart, or in and around the lungs. Dyspnea can also be caused by increased intra-abdominal pressure (by ascites or a large tumor mass).

Table 2 (continued) | Clinical signs associated with cancer models: description, recognition and etiology

Clinical sign	Description	How to assess?	Etiology
Respiratory signs (Continued)			
Tachypnea	Increased breathing frequency	Normal respiratory rate for most rodents is 120–240 respirations per minute. Although difficult to count, with experience tachypnea can be detected. Automated assessment of respiratory rate and/or movement in automated cages is possible, but requires solitary housing and specialized equipment[28,193].	
Hypoxemia	Decreased oxygen concentration in blood	Can be observed as cyanosis, i.e., blue discoloration of mucous membranes and skin. Desaturation can be measured with a pulse oximeter.	Hypoxemia is caused by anemia or dyspnea.
GI signs			
Diarrhea	Increased frequency and/or decreased consistency of stool (i.e., loose stool)	Feces look less firm. Depending on the severity of the diarrhea, feces may become pasty, semiliquid or watery.	Occurs mostly in tumors of the GI tract. The specific sign depends on the tumor location and model e.g., diarrhea and bloody stool are common in colorectal cancer models, constipation can be caused by luminal occlusion but can also be seen in dehydration (see above). GI signs are also known side-effects from many chemotherapeutics or other cancer treatments such as radiation therapy. Diarrhea is also a known side-effect from GVHD[181].
Bloody stool	Passage of fresh blood through the anus due to bleeding in the lower part of the intestines	Fresh (red) blood seen in/on the feces.	
Rectal prolapse	Eversion of the rectal mucosa from the anus	It presents as a small red mass at the anus.	
Constipation	Infrequent or difficult evacuation of feces	In mice, this can be presented by an enlarged abdomen, absence of defecation when handled and/or a decreased amount of fecal pellets present in the cage.	
Urinary signs			
Hematuria	Urine containing red blood cells	Gross hematuria can be seen during urination upon manipulation and/or the presence of discolored (red-tinged) contact of clear (pink) blood in the bedding or urine when using metabolic cages.	May be seen in models of bladder cancer as a consequence of blood loss of the tumor.
Urinary retention and obstruction	Urinary retention: condition in which urine cannot completely be emptied from the bladder Urinary obstruction: condition in which urine flow is completely blocked	Mice frequently urinate during handling and abdominal palpation. With urinary retention or obstruction, mice will not urinate and manual expression of the bladder is difficult or impossible[184]. In severe cases, a bulge or swelling can be observed in the caudal abdomen and an enlarged bladder can be detected upon abdominal palpation. Urinary retention or obstruction often leads to hydronephrosis (i.e., swelling of the kidneys), which can be palpated in the dorsal abdomen. In males, a distended and/or an abnormally colored penis (dark red to purple) probably indicates urinary obstruction.	In models requiring estrogen supplementation, urinary retention and other urinary signs are well-known side-effects[194,195] and care should be taken to prevent their occurrence (see Table 10, monitoring sheet for urinary signs). Urinary obstruction is caused by a blockage or narrowing of the bladder, ureters or urethra by a mass.
Polyuria and polydipsia	Polyuria: excessive or abnormally large production and/or passage of urine. Polydypsia: excessive drinking caused by increased thirst	When mice/rats urinate more, the bedding will become wetter. Polydypsia can be assessed by the water bottle, which will empty more rapidly.	Polyuria and polydipsia are associated with various tumor types (e.g., kidney, adrenal, pancreatic) by causing a hormonal or electrolyte disbalance, which can alter body fluid retention and excretion.
Neurological signs			
Circling and rolling	Neurological signs indicating abnormal and uncontrollable movement of the animal around one of the body axes	Circling: animal walks in circles always in one direction (usually the same side as the lesion). May be associated with a head tilt in the same direction. Rolling: rapid movement in a tight circle, with the animal actually turning on itself.	Neurological signs may occur due to invasion or compression of the brain or other parts of the central or peripheral nervous system by a tumor or tumor cells (e.g., leukemia). The specific signs depend on the area that is affected.
Head tilt	Abnormal position of the head turned to one side	The head is tilted towards the left or the right.	
Paresis/ paralysis	Paresis: weakening of a muscle or group of muscles due to nerve damage or disease Paralysis: complete loss of the function of a body part or parts	In advanced stages, these signs will be obvious on visual assessment. In earlier stages, the following (easy to perform) tests may aid in determining early stages of paresis/paralysis and ataxia[196–199]. Clasping test: when lifting a mouse or rat by its tail it should spread its legs away from the abdomen. Retracting (one of) its limbs towards the abdomen is called clasping. Grip test: the mouse or rat should grip the bars of a cage lid when placed on the grid and pulled slightly back by its tail. Kyphosis test: placing the mouse on a flat surface and observing it while it walks, it should be able to straighten its spine. Not being able to do so is called 'kyphosis' (kyphosis is only validated in mice; however, it can also be used in rats).	
Ataxia	Loss of coordination during movement		

Table 2 (continued) | Clinical signs associated with cancer models: description, recognition and etiology

Clinical sign	Description	How to assess?	Etiology
Neurological signs (Continued)			
Epileptic seizures	Sudden and uncontrolled electrical disturbance in the brain, which causes the animal to suddenly change its behavior and movements	Often observed as uncontrolled spasms and being disconnected from its environment. This is usually seen during animal manipulation or cage change.	
Locomotor signs			
Lameness	Inability to walk normal caused by either a structural or a functional disorder of the locomotor system	Observed as an abnormal gait.	Occurs most commonly as a result of local pain caused by inflammation or from a growing tumor in an area with limited capability to accommodate expansion, e.g., in bone. May also result when the tumor mass interferes with movement of a limb or impedes lymphatic flow resulting in swelling as a result of edema.

Other implantation sites, e.g., around the head, footpad and inside of the thigh should be avoided unless there is particular scientific purpose. In general, a single site should be used; however, no more than two sites should be implanted. Implanting more than one tumor per flank will increase the risk of side effects such as locomotor issues in case tumors are implanted further apart from each other or fusion of the different tumors if implanted too close to each other. Furthermore, scientifically there is usually no added value of implanting more than two tumors.

Mammary gland tumor transplantation. Tumors should preferentially be implanted in the third or fourth mammary glands as these sites are less likely to cause site-related morbidity or interfere with normal body functions. The most cranial (first) and caudal mammary glands (fifth in mice, sixth in rats) should be avoided, unless there is a clear scientific need, as growth at this site can hamper movement of the animal. Depending on the research question, a specific mammary gland can be better suited than another[69]. Implantation in the mammary fat pad can be refined by using a technique wherein the mammary fat pad is no longer cleared for endogenous mammary tissue and tumor cell suspension is injected by slightly pulling out and exposing the fat pad through an incision size <3 mm instead of through a large V-shaped incision[72]. A variety of injection volumes have been reported; however, the maximum volume of Matrigel or Cultrex to be injected in the mammary fat pad of mice without spillage is 20–30 µl (second to fourth mammary fat pad, respectively)[73]. In case of tissue fragment transplantation, fragments should not exceed 3 × 3 mm (ref. 74). Intraductal injection does not necessitate cutting the teat. A stereoscope and fine needle (30–34G) should be used to inject tumor cells directly into the teat canal. Dead skin covering the teat canal opening should be removed to facilitate insertion of the needle[75]. In mice, volumes of 10–20 µl can be injected intraductally[75]. In rats, 60 µl can be injected as the ductal tree is much larger[76]. Overall, no more than two mammary glands should be implanted.

Intracerebral tumor implantation/injection. Injection or implantation into the cranium requires the use of a stereotaxic frame. Stereotactic surgery can be refined by using appropriate multimodal analgesia including local anesthesia prior skin incision (of note: local anesthetics containing adrenalin will diminish intra-operative bleeding). Ear bars not puncturing the tympanic membrane should be used[77,78]. The implantation site can have an important effect on tumor growth, survival and histologic characteristics and therefore must be carefully considered[79]. Especially in rats where skull thickness can vary as a function of age, the reference point for the calculation of the depth can be taken from the dura[78]. Needles specifically designed for intracranial use allow the delivery of microvolumes while minimizing tissue damage. Consider wiping the needle tip before needle positioning for aggressive cell lines to ensure no tumor cells adhere to the surrounding skull. Following needle insertion, allow 1–2 min for brain tissue to acclimatize. Reduce the volume of injection to the minimum with a maximum of 5 µl at maximum speed of 1 µl/min. Following completion of injection, allow tumor cells to accumulate in the bottom of the needle tract for 1–2 min, before slow needle withdrawal. Washing the skull (with 0.9% NaCl) will avoid ectopic tumor growth.

Intrapulmonary tumor implantation. To develop orthotopic lung cancer models, tumor cells have been injected in the lung percutaneously[80,81]. However, this surgical technique can lead to major adverse effects including thoracic bleeding and pneumothorax[81]. In contrast, the implantation of cells through the trachea prevents the development of such undesired adverse effects. Administration of cells in the trachea can be achieved through surgical tracheostomy[82]. However, nonsurgical instillation based on standard intubation methods for rodent ventilation[83,84] is the most refined and thus preferred technique. Nonsurgical instillation results in a single well-defined tumor instead of multifocal lesions[83,84], making tumor measurement easier and more accurate. Several aids are described to facilitate the visualization of the vocal cords: a fiberoptic light[85], an intubation standard[83], a surgical microscope[84] or an external light source[86] (the choice which can be based on personal preference). To avoid damage of the laryngeal structures and obtain optimal refinement, cannulae should be as atraumatic and small as possible. Therefore, it is preferable to utilize a plastic (e.g., intravenous catheter) rather than a metal cannula. Moreover, it is important to have sufficient experience to intubate and ensure minimal trauma quickly and proficiently. The length of the cannula should be adapted to the size of the mice to avoid puncturing the lung. The maximum cell suspension recommended for intratracheal injection is 30–50 µl for mice and neonatal rats, and 100 µl for adult rats.

Tumor implantation into the abdomen. Orthotopic implantation of cancer cells and/or tissue into the abdominal organs (intestines, pancreas, liver, urogenital organs) may require laparotomy. Standard refinement for surgical procedures are described in Box 3. When performing a laparotomy, ensure incision length is minimized.

Table 3 | Monitoring of tumors

Tumor type	What to monitor?	Method				Frequency	Criteria for killing	Refs.
		How?		Advantages	Disadvantages			
		Visual inspection and palpation						
Cutaneous tumors (SC, mamma and melanoma)	Tumor volume	Caliper	Correctly position caliper at widest, longest and deepest tumor region Gentle manipulation is required and no direct pressure should be placed on tumor See Box 1 for correct placement of caliper	Noninvasive with minimal impact on animal welfare	Moderate reproducibility and accuracy (compared with imaging) Cannot distinguish between living and necrotic cells	Begin once palpable tumors are present; 1–2 times per week depending on tumor growth rate. Frequency to increase as animal approaches endpoint (at least 3 times per week or daily)	Total tumor volume of 2 cm^3,[a] for mice and 4 cm^3 for rats. Tumor touching the cage floor in case of ventral location Ulceration (Table 12)	200,201
Oral cavity		Visual inspection and palpation	Using forceps and light pressure, gently withdraw the tongue. For larger tumors, animals are placed in a supine position	Clear protocol No specialized material required	Immobilization by anesthesia required Small inspection field Low reproducibility and accuracy	At least 2 times per week. Frequency to increase as animal approaches endpoint	Unable to eat, drink and/or groom due to pain and/or obstruction Bleeding tumor	202,203
Intra-abdominal		Palpation	Place the mouse or rat on the cage grid and gently lift by the tail Palpate the abdomen by smoothly going up and down with index and thumb of the nonfixing hand If soft palpation is tolerated, proceed by slowly increasing the pressure. A larger resistance can easily be detected in the upper and/or lower abdomen Use a scoring system based on tumor size relative to the mouse/rat hemi-pelvis or midline (zero = nonpalpable, 1 is <25%, 2 is 26–49% and 3 is >50%)		Experience needed Only for solid tumor masses Low reproducibility and accuracy	1–2 times per week depending on growth rate of the tumor; increase near endpoint	Pain reaction upon palpation Tumor mass with score 3 (>50%) Correlate prior- and postnecropsy measurements to determine HEPs for future studies	25, 204,205
Hemato-poietic			Restrain the mouse and place in a supine position The spleen, located in the left quadrant, can be palpated with the index and thumb of the nonfixing hand Use a scoring system based on extension of the spleen (0.5 = normal spleen; 1 = spleen extends halfway between left rib cage and first quadrant line; 2 = spleen extends to the median line; 3 = spleen extends halfway between median line and right rib cage; 4 = spleen extends to the right rib cage)		Experience needed Only for hematopoietic tumors associated with splenomegaly Low reproducibility and accuracy		Spleen extending to the right quadrant (score ≥3)	206

https://doi.org/10.1038/s41596-024-00998-w

Table 3 (continued) | Monitoring of tumors

Tumor type	What to monitor?	Method				Frequency	Criteria for killing	Refs.
		How?		Advantages	Disadvantages			
		Endoscopy						
Esophagus Colorectal	Volume and luminal occlusion	Endoscopy	Use a small endoscope to visualize distal colon and esophagus lumen Evaluate ulceration, inflammation and bleeding Assess tumor(s) on size, number and luminal occlusion	Possibility to take biopsies and pictures	Experience needed Immobilization by anesthesia Resource intensive by specialized equipment	Frequency of imaging depends on study design and limitations of general anesthesia frequency allowed by regulatory authority	Luminal occlusion of 50% or more. Inability to pass food/feces	140, 207–211
		Blood and urine analysis						
Hemato-poietic	Percentage human leukemic cells in blood	Blood sampling	Use flow cytometry to define % of leukemic cells (e.g., human-specific markers in PDX models or GFP-labeled tumor cells)	Accurate and reproducible method	Blood volume may be a limiting factor in mice. Using micro-sampling and correct hemostasis techniques may overcome this issue	Every 2 weeks; increase as animal approaches endpoint	Significant difference between models and therefore not possible to provide exact quantification	
	Total white blood cells		Measure total white blood cells to assess disease progression usually through a hematology analyzer				Correlate white blood cell counts and/or % leukemic cells with deterioration of mouse/rat condition to determine HEPs for future studies	212
Transdu-cable cell lines	Secreted Gluc reporter in blood, serum or urine	Gluc reporter assay	Gaussia luciferase or Gluc are naturally secreted reporters Can be used as markers to monitor tumor growth and therapeutic response Linearity between Gluc reporter signaling and cell number Easily monitored by withdrawing few microliters of blood and assaying for activity, allowing real-time follow-up of in vivo processes Can be used in combination with bioluminescence to localize tumors	Assay completed in minutes Very short half-life No need for expensive instrumentation	1.000-fold more sensitive compared with secreted alkaline phosphatase reporter assay; therefore, prone to errors Affection of the Gluc signaling by neutralizing antibodies in experiments >3 weeks	Every 3 d over the course of a month	Correlate Gluc reporter signaling with in vivo bioluminescence to determine HEPs for future studies	213

https://doi.org/10.1038/s41596-024-00998-w

Table 3 (continued) | Monitoring of tumors

Tumor type	What to monitor?	Method					Frequency	Criteria for killing	Refs.
		How?		Advantages	Disadvantages				
		Anatomical and molecular imaging							
Cutaneous tumors	Volume	Three-dimensional (3D) through biovolume	BioVolume combines thermal and photographic images to calculate tumor volume. Modality currently only validated for mouse tumors	Rapid imaging Minimally invasive Morphology-independent Reduction of human bias	Immobilization by anesthesia required Resource intensive as specialized equipment is required Expertise in imaging and image analysis required	Requires specialized BioVolume scanner	Start as soon as palpable tumors are present; 1–2 times per week depending on growth rate of the tumor; increase near endpoint to at least 3 times per week or daily	Total tumor volume of 2 cm^3,[a] (mice) Tumor in ventral location touching the cage floor Ulceration (Table 11)	214
Firefly-luciferase cell lines/ tumors	Light emission	Bioluminescence	Biological light emission Generation of a photon flux (light) when luciferin is oxidized by the firefly reporter enzyme luciferase in the presence of ATP Gently restrain mouse/rat and administer luciferin via the appropriate route	Highly sensitive method with minimal background signal Can be used to detect metastasis Only living tumor cells detectable		Low accuracy of tumor volume Only tumor cell lines or mouse/rat models constructed to express luciferase are detectable Lack of an anatomical reference frame available, complementary imaging modality needed Light scattering caused by fur; need for hair removal	Frequency of imaging depends on study design and limitations of general anesthesia frequency allowed by competent authorities Weekly imaging typically suitable	As it is impossible to measure exact tumor volume, criteria for killing based on tumor volume are unavailable Imaging modalities can however aid in defining HEPs for future studies as emission values can predict deterioration of mouse/rat condition, metastasis and tumor volume	215–218
Fluorescent cell lines/ tumors	Fluorescent light emission	Fluorescence imaging	Living cells labeled with a fluorescent molecule (e.g., GFP) emit a specific wavelength of light upon excitation via electromagnetic radiation	Can be used to detect metastasis Possible to gain information on single-cell level Varying cell types can be labeled in different colors		Only tumor cell lines or mouse/rat models constructed to express a fluorescent protein with wavelengths compatible with in vivo tissue imaging are feasible for use (>650 nm) Modality lacks an anatomical reference frame, therefore a, complementary imaging modality is required Background auto-fluorescence may interfere with signal. Background signal can be limited through the use of a 'low fluorescent' diet. Limited by low fluorescent diet			219–222
Orthotopic tumors	Volume	Computed tomography (CT) and contrast-enhanced CT (CE-CT) imaging	CT: ionizing radiation from different angles produce cross-sectional images CE-CT: administer iodine-based contrast agents via oral gavage, intraperitoneal or i.v. injection to allow tumors to be visualized via negative or positive contrast	Measurement of exact tumor volumes possible High resolution, very sensitive Short imaging time Possible to generate 3D images of tumor Facilitates monitoring of luminal occlusion of colorectal and esophageal tumors		Potential impact of radiation on tumor growth	The use of ionizing radiation restricts the use of CT Frequency of imaging depends on study design and limitations of general anesthesia frequency allowed by regulatory authorities	Lung: tumor composes max 50% of the total lung volume Bone and muscle: max 10 mm tumor diameter in mice; max 15 mm tumor diameter in rats. Brain: max 25% of the total volume (±500 mm^3 in mice depending on the strain)	201, 223,224

https://doi.org/10.1038/s41596-024-00998-w

Table 3 (continued) | Monitoring of tumors

Tumor type	What to monitor?	Method		Advantages	Disadvantages	Frequency	Criteria for killing	Refs.
		How?						
		Anatomical and molecular imaging (continued)						
				CE-CT facilitates the visualization of intra-abdominal tumors, such as liver or colorectal tumors that have a similar X-ray absorbance to the surrounding tissue Use of blood-pool contrast allows visualization of liver metastasis CT radiomics can be applied to images: radiomics involves the extraction of large numbers of radiographic features from images based on shape, pixel intensities, and texture			Abdominal tumors: should not exceed 1.5 cm^3 in volume in mice, 3 cm^3 in rats Luminal occlusion of 50% or more; inability to pass food/feces Detection of metastatic lesions with criteria tailored to study design	
Soft tissue and bone		Magnetic resonance imaging (MRI)	The use of strong magnetic fields to generate images of soft tissues and bone tumors	Allows measurement of exact tumor volumes Possible to generate 3D images MRI radiomics can be applied to images	Lengthy procedure thus requiring long anesthesia Follow-up of intrathoracic tumors requires specialized gating	Frequency of imaging depends on study design and limitations of general anesthesia frequency		225–228
Intra-abdominal and lung		Ultrasound	Sound waves are reflected by the tissues with different properties. Ultrasound waves are therefore used to acquire images		Less suitable for imaging of large areas, whole body or metastasis			204, 229–231
Radio-labeled cells and tumors	Tumor-specific biomarkers and emission of gamma rays	Positron emission tomography (PET)/single-photon emission computed tomography (SPECT)	Visualization of molecular aspects and metabolic alterations in highly metabolically active tumor cells upon injection of radioactive tracers	A novel method for staging and classification of tumors Assist in determining response to treatment Provide hints toward improved understanding of tumor biology Possible to detect metastasis Visualization of different aspects of the tumor depending on the tracer PET radiomics can be applied to the images	Lack of an anatomical reference frame, therefore complementary imaging (CT/MRI) modality needed Inter-institutional differences in imaging acquisition and processing Differences between clinical and preclinical scanners Unable to exactly measure tumor volume Depending on the half-life of the tracer, animals and their excretions may be radioactive after imaging Requires fasting to lower blood glucose levels as this could interfere with radiotracer signal	Frequency of imaging depends on study design and limitations of general anesthesia frequency allowed by competent authorities As the use of ionizing radiation and tracers limits the use, the frequency should be adapted accordingly	As it is not as sensitive as CT or MRI, criteria for killing based on tumor volume are difficult to define Imaging modalities can, however, aid in defining HEPs for future studies as emission values can predict deterioration of mouse/rat condition, (distant) metastasis and tumor volume	216, 232–234

[a]It is generally not necessary to go beyond 1.5 cm^3 in mice to obtain enough scientific data.

https://doi.org/10.1038/s41596-024-00998-w

https://doi.org/10.1038/s41596-024-00998-w

Table 4 | General animal monitoring sheet

Parameter	Outcome	Actions to be taken
Anorexia and BW loss[a]		
BW loss[b]	<5%	None
	5–15%	Increase general monitoring frequency to 3 times per week. As soon as animals start to lose weight, providing extra nutrition may avoid extra weight loss and premature killing (Fig. 2)
	16–20%	Increase general monitoring frequency to 1 time per day to avoid exceeding 20% BW loss Increase skin turgor test frequency to daily (Table 2). If dehydrated, see Fig. 2. If dehydration persists despite treatment: humane killing
	≥20%	Humane killing
OR[a]		
BCS[182,183]	3 or 4	None
	2	Increase general monitoring frequency to 1 time per day to avoid progress to BCS 1 Increase skin turgor test frequency to daily (Table 2). If dehydrated, see Fig. 2. If dehydration persists despite treatment: humane killing
	1	Humane killing
Hydration[a]		
Skin turgor test (Table 2)	Negative	None
	Positive	If dehydrated, see Fig. 2. If dehydration persists despite treatment: humane killing
Appearance and behavior[c]		
Posture	Hunched—on one occasion	Increase general monitoring frequency to 3 times per week
	Hunched—on two consecutive occasions	Increase general monitoring frequency to 1 time per day
	Hunched—more than 7 d	Humane killing
Fur	Ruffled	Increase general monitoring frequency to 3 times per week Ruffled without other signs is usually not a direct criterium for killing
Activity	Mildly decreased; less interactive	Increase general monitoring frequency to 3 times per week
	Stationary until stimulated; isolated or hyperactive	Increase general monitoring frequency to 1 time per day
	Unresponsive/lethargic	Humane killing
Pain[c]		
Pain	Present or likely	Provide appropriate (multimodal) analgesia[d] Increase general monitoring frequency to at least daily or more often when analgesics are provided more often
	Present despite analgesia	Humane killing

[a]Assess 1 time per week; increase if necessary (see actions to be taken). [b]See Box 4 for the relation between body and tumor weight. [c]Assess 2 times per week; increase if necessary (see actions to be taken). [d]Analgesic treatment usually does not alter tumor growth patterns[235–237] and should be provided when animals experience pain. Only if there is direct evidence of interference with the model an alternative plan to alleviate pain/distress must be identified in consultation with veterinary staff.

Table 5 | Monitoring sheet for animals undergoing surgery

Parameter	Outcome	Actions to be taken
Surgical wound		
Wound dehiscence without opening of body cavity	Wound margins dry and crusted	Treat with wound healing gel or cream[a] at least once daily and allow spontaneous healing[b]. If no clear improvement after 5 d: humane killing Analgesia should be given when signs of pain or inflammation are present
	Wound margins 'fresh'	Reclose the wound[b]. If opening is small (1–2 stitches): use tissue glue (usually no anesthesia necessary). If large: anesthetize the animal and resuture Analgesia should be given when signs of pain or inflammation are present
Wound dehiscence with opening of body cavity	—	Humane killing
Infection	Local	Apply antibiotic cream if the protocol allows[b]
	Generalized	Provide systemic antibiotics if the protocol allows[b] Humane killing when no improvement after 48 h of treatment or if treatment is not allowed by the study protocol
Pain		
Pain	Present	Provide analgesia
	Present despite analgesia	Add extra analgesia
	Present despite multimodal analgesia	Humane killing

Assess daily for 3 days postoperative. Increase or prolong if necessary (see actions to be taken). [a]For example, enzyme alginogels[238] or honey cream[239]. [b]In consultation with the facility veterinarian.

Table 6 | Monitoring sheet for animals with tumors causing respiratory signs

Parameter	Outcome	Actions to be taken
Breathing		
Frequency	Normal	None
	Tachypnea	Increase general monitoring frequency to 1 time per day
Pattern	Normal	None
	Dyspnea	Humane killing
	Gasping	Humane killing
Oxygen saturation		
Color of mucous membranes	Pink	None
	Cyanosis	Humane killing
Stress test		
Stress test[a] (Fig. 3)	Negative	None
	Positive: distress in >3 s	Increase general monitoring frequency and stress test to 2 times per day
	Positive: distress in <3 s	Humane killing

Assess 3 times per week; increase if necessary (see actions to be taken). [a]The stress test has so far only been validated in mice.

Table 7 | Monitoring sheet for animals with tumors causing neurological signs

Parameter	Outcome	Actions to be taken
Neurological signs: visual assessment of animals in cage		
Circling and head tilt (note that these may worsen or only become apparent when animals are manipulated)	Present but still able to move around the cage and reach food and water	Increase general monitoring frequency to 1 time per day. Adding easy to reach food may prevent weight loss
	Circling and/or head tilt preventing animals to eat and/or drink	Humane killing
Paresis/paralysis and ataxia	Present but still able to move around the cage and reach food and water	Increase general monitoring frequency to 1 time per day. Adding easy to reach food may prevent weight loss
	Severe paresis/ paralysis/ataxia preventing animals to eat and/or drink	Humane killing
Seizures	Present	Humane killing
Neurological signs: neurological tests		
Grip, clasping and kyphosis test (Table 2)	Positive test	Increase general monitoring frequency to 1 time per day. Adding easy to reach food may prevent weight loss
	Severe paresis/ paralysis/ataxia preventing animals to eat and/or drink	Humane killing

Assess 3 times per week; increase if necessary (see actions to be taken).

Handle all abdominal organs, particularly the intestines, gently using nontraumatizing instruments or cotton buds and avoid the application of pressure to the organs. Inappropriate/rough handling may induce ileus or other gastrointestinal (GI) problems. When organs are exteriorized (placed outside the body cavity), maintain moisture by applying warm sterile NaCl solution. Gently reinsert the organs into the abdomen following cell-suspension injection or tumor-fragments implantation before closing the abdominal wall in two layers (peritoneum/muscle and skin) Avoid accidental spillage of cells into the abdominal cavity by injection of the appropriate volume and use a proper gauge needle, depending on the species and organ. The use of a dissecting microscope may assist in visualization. A laparotomy is a painful procedure[87] so apply appropriate multimodal analgesia for minimum 48–72 h following surgery. Other than laparotomy, implantation in abdominal organs can be achieved through non- or minimally invasive and thus more refined

Table 8 | Monitoring sheet for animals with tumors causing locomotor signs

Parameter	Outcome	Actions to be taken
Abnormal gait: lameness	Abnormal gait caused by tumor location (e.g., mammary or edema due to lymph blockage)	Increase general monitoring frequency to 1 time per day. Adding easy to reach food may prevent weight loss
	Intermittent use of affected limb, protective pose or tip-toed walk caused by pain or inflammation	Provide analgesia[a]
	Persistent lameness despite analgesia	Humane killing
	No weight bearing (no use of affected limb)	Humane killing

Assess 3 times per week; increase if necessary (see actions to be taken). [a]In consultation with the facility veterinarian.

Table 9 | Monitoring sheet for animals with tumors causing GI signs

Parameter	Outcome	Actions to be taken
Stool consistency	Normal	None
	Diarrhea or loose stool	Increase general monitoring frequency to 1 time per day Start checking hydration (skin turgor test, Table 2). If dehydrated, see Fig. 2. If dehydration persists despite treatment: humane killing
Bloody stool	Present	Increase general monitoring frequency to 1 time per day Start checking for anemia daily (Table 2). If anemia: humane killing
Rectal prolapse	Present but limited in size, not bleeding, mucosa is pink and wet, animal can still defecate[a]	Increase general monitoring frequency to 3 times per week
	Present and dry or necrotic, bleeding, getting bigger or impossible to defecate	Humane killing
Constipation	Present	Increase general monitoring frequency to 1 time per day Provide macrogol through the drinking water[b] If constipation persists, humane killing

Assess 2 times per week; increase if necessary (see actions to be taken). [a]Mitchell et al. have demonstrated that treatment of rectal prolapse in mice is not necessary and that mice with rectal prolapse do not show signs of pain or distress[240]. [b]Dissolve macrogol (13.9 g/25 ml) in the water bottle (replace once/week). Best results are obtained when macrogol is given as a preventive measure (i.e., when compounds are known to cause constipation) (J. Verbeeck, personal communication).

Table 10 | Monitoring sheet for animals with tumors causing urinary signs

Parameter	Outcome	Actions to be taken
Hematuria	Present without anemia	Increase general monitoring frequency to 1 time per day
	Present with anemia	Humane killing
Urinary retention[a]	Present	Increase general monitoring frequency to 1 time per day. Check if manual expression of the bladder is possible. If no: humane killing. If yes: express the bladder at least two times a day. If no amelioration after 48 h: humane killing
Polyuria	Present	Increase general monitoring frequency to 1 time per day. Start checking hydration (skin turgor test, Table 2). If dehydrated, see Fig. 2. If dehydration persists despite treatment: humane killing. Make sure bedding and water bottles are replaced more frequently (at least 2 times per week)

Assess 2 times per week; increase if necessary (see actions to be taken). [a]Urinary retention, a known side-effect from estrogen supplementation[194,195], can be avoided by adding estrogen through drinking water instead of via pellets[241].

https://doi.org/10.1038/s41596-024-00998-w

Table 11 | Monitoring sheet for animals with tumors causing ascites

Parameter	Outcome	Actions to be taken
BW	BW loss of >10% in 2 d or >15% in 1 week during development of ascites	Humane killing
Abdominal distention	Present	Increase general monitoring frequency to 1 time per day and start weighing animals daily
	Abdominal distention causing discomfort, dyspnea or interference with normal activity[a]	Perform ascitic tap. A maximum of three taps is allowed. From now on, animals should be monitored and weighed at least daily
	Abdominal distension causing discomfort/ interference with normal activity after the final tap	Humane killing
	Abdominal distention causing discomfort or interference with normal activity that cannot be relieved by ascitic tap	Humane killing
Ascitic tap	Signs of shock (tachypnea, hunched, pale ears/muzzle/tail, inactivity) after tap	Give 100 ml/kg warmed saline SC in multiple sites and put the animal on a heating pad, observe for 30 min
	Signs of shock (tachypnea, hunched, pale ears/muzzle/tail, inactivity) lasting >30 min after tap	Humane killing
	Purulent fluid	Humane killing

Assess 3 times per week; increase if necessary (see actions to be taken). [a]In a well-defined model, discomfort usually develops at a specific body-weight (e.g., 32 g in the model used by Baert et al.[158]). A pilot study can aid in determining this value.

methods. For intestinal tumors, nonsurgical implantation in the distal rectum[88,89] or implantation through endoscopy[90] have been described. Hite et al. compared the intrarectal (not requiring laparotomy) and intracecal injection performed via laparotomy. While the intrarectal injection group had a mortality rate of 4%, the mortality rate in the intracecal injection group was 17%. Both methods had a 100% tumor uptake[91]. Also for implantation in the liver, spleen, pancreas, adrenal and subcapsular region of the kidney, alternative and more refined injection methods through ultrasound guidance have been validated thereby avoiding the more invasive injection method through laparotomy[92–95]. Tumor take rates were high (up to 100%) in all organs and authors stated the procedure to be short and easy to perform. For inoculation in the bladder, both injection through ultrasound guidance[96] as well as transurethral injection[97,98] do not require a laparotomy.

Intravenous tumor injection. Typically, the lateral tail vein is used for intravascular delivery of agents in rodents. Similar principles apply for intravenous injection of tumor cells as for intravenous injection of other compounds. Briefly: use the smallest needle possible (may depend on tumor cell size), preheat the tail of the animal to ±37 °C to promote peripheral vasodilatation and use the correct restrainer. A useful alternative to tail vein injection is the technique of retro-orbital injection of the venous sinus in the adult and neonatal mouse. This easily mastered technique is a refined method for bone marrow transplantation, leukemia induction, administration of experimental compounds and gene therapy, creating less distress with a lower failure rate[99,100]. Note that although bone marrow cells have traditionally been injected intravenously, engraftment of bone marrow cells have a higher success rate when injected directly in the bone marrow[101,102] (see below).

Table 12 | Monitoring sheet for animals with cutaneous ulcerating tumor

Parameter	Outcome		Actions to be taken
Tumor aspect	No lesion (score 0)		No treatment required
	Redness at the site of the tumor, skin still intact (score 1)		
	Skin open but 'dry' (top image), no discharge present. A scab (bottom image) can be present (score 2)	 	Start daily monitoring. Treatment with wound healing gel or cream[a] is recommended. This could prevent the ulceration to further evolve
	Skin open and wet. Purulent or bloody discharge is present (score 3)		Humane killing if ulceration does not dry up within 72 h Treatment with wound-healing gel or cream[a] is highly recommended and could prevent necessity for humane killing In case of infection (purulent discharge) antibiotic cream can be necessary Provide analgesia[b]

Assess 2 times per week; increase if necessary (see actions to be taken). [a]Such as enzyme alginogels[238] or honey cream[239]. [b]In consultation with the facility veterinarian. Images provided by The Netherlands Cancer Institute.

Table 13 | Severity assessment of cancer models based on clinical consequences, implantation method and tumor characteristics (regardless of their origin)

		Mild	Moderate	Severe
Clinical consequences	BW loss and BCS	BW loss up to 10% BW loss of 10–15% loss >7 d	BW loss of 10–15% loss ≤7 d BW loss of 15–20% loss >2 d Animals with BCS 2	BW loss of 15–20% loss ≤2 d BW loss of >20% loss Animals with BCS 1 All models of cancer cachexia
	Neurological signs	Animals with circling/head tilt/ataxia not preventing them to eat/drink	Animals culled as soon they develop: seizures, paresis/paralysis, ataxia/head tilt/circling preventing animals to eat/drink	—
	Ascites, icterus, anemia	—	Animals culled as soon they develop ascites, icterus or anemia	Models requiring ascitic tap
	GI signs	—	Animals with: diarrhea without dehydration, rectal prolapse, bloody stool, constipation	—
	Dehydration	—	—	Animals remaining dehydrated despite treatment
	Respiratory signs	—	Animals with tachypnea	Animals with dyspnea, cyanosis or positive stress test
	Locomotor signs	—	Animals with lameness	—
	Urinary signs	—	Animals with urinary retention, hematuria or polyuria	—
	Pain	—	—	Animals with pain despite analgesia Models of cancer pain Bone tumor models
	Moribundity/mortality	—	—	Moribund animals or animals found dead
Tumor characteristics	—	Uncomplicated SC, mammary or skin tumor ≤2 cm^3 in mice, ≤4 cm^3 in rats	Ulcerated SC, mammary or skin tumor Other uncomplicated tumors reaching maximum size as defined in Table 3 (note that bone tumors are always severe)	—
Implantation method	—	SC implantation	Implantation requiring major surgery or repeated surgery (recurrent model) or implantation through HDTVI	—

HDTVI. Hydrodynamic tail vein injection (HDTVI) is a technique wherein a high volume (up to 10% of BW) of a (cell/vector/plasmid) suspension is rapidly (usually within no more than 10 s) injected intravenously to facilitate uptake of tumor cells in the liver. HDTVI causes a massive expansion of the liver, an increase in pressure in the vena cava and massive drop in arterial pressure accompanied by electrocardiogram abnormalities. High injection volumes can cause respiratory arrest[103,104]. Therefore, close monitoring post procedure is mandated (at least 1 h after injection) and analgesics are required. The use of anesthesia for HDTVI is under debate as it may increase mortality.

Intracardiac tumor injection. Intracardiac injection may be used to study brain or bone metastasis. This technique, however, entails a substantial risk of mortality. Campbell et al. describe how this injection should be performed technically[105]. Using ultrasound guidance to correctly position the needle will increase success rate and decrease mortality[94,106]. Some (larger) tumor cells may cause thrombo-embolism and injecting a low-molecular heparin intravenously before intracardiac injection will reduce this risk[107].

Intramuscular tumor implantation/injection. Implantation in the muscle should be avoided whenever possible. Muscle distention is painful and there is a risk of affecting locomotion. A maximum of 50 µl should be injected with the finest needle possible (e.g., 27G or smaller) in the quadriceps or caudal thigh muscle[108].

Intrabone marrow/intra-osseous tumor injection. Recent evidence has demonstrated that intrafemoral injection in mice significantly decreases the degree of impairment and distress postoperative compared with intratibial injection[109]. Nevertheless, when performing an intratibial injection, a 30G (rather than 26G) needle is recommended as a refinement. Moreover, the patellar tendon should be avoided[109]. The risk of impairment and lameness dictates that intrabone marrow transplantation should be limited to one leg per animal. In bone tumor models, intra-osseous implantation (versus para-tibial) results in a more clinically faithful disease model, despite a potentially reduced tumor growth. Nevertheless, this method is frequently associated with a dissemination of cells in the bloodstream, which can be partly prevented by slowly retracting the needle after injection and reducing the number of cells injected[110].

Para-tibial tumor implantation. To stimulate seeding of the tumor cells, the periost should be activated with the tip of a needle (periosteum denudation). Use the finest (e.g., 30–31G) needle possible to avoid soft tissue injury and inflammation as much as possible[110]. Note that the periost is very sensitive and sufficient analgesia should thus be provided.

Carcinogenic tumor models. More than in implanted tumors, carcinogen-induced tumors may occur unpredictably in terms of timing, location and number of lesions. Variable responses to carcinogens may not only depend on type and dosage of carcinogen but also on strain,

BOX 2

Appropriate anesthesia and aseptic surgery

Appropriate anesthesia, analgesia and perioperative care enhances animal well-being and improves experimental quality. Anesthetic and analgesic regimens have been described elsewhere[242–244] and are beyond the scope of this manuscript. However, the following principles should be applied. Anesthetic depth and duration should be appropriate to the scope and duration of the procedure. Painful procedures must only be performed when achieving surgical plane of anesthesia (i.e., pain reflexes absent). Preemptive and multimodal anesthesia and analgesia should be employed. Preemptive refers to the administration of analgesics before the painful insult to minimize postprocedure pain. This is usually given at the time of anesthetic induction. Multimodal anesthesia and analgesia refers to the use of different pharmacological classes of anesthetics and analgesics to minimize pain, e.g., by combining local anesthesia at the site of incision and systemic administration of opioids and nonsteroidal anti-inflammatory drugs. Importantly, frequently used anesthetics in rodents (e.g., gas anesthesia) have generally no or minimal analgesic properties and therefore require the use of additional analgesics.

Animals undergoing surgery must receive effective perioperative care. In the preoperative period this mainly consists of preemptive analgesia and proper planning and preparation. During surgery, appropriate measures should be taken to avoid infection and aseptic techniques should be utilized. Animals should be kept warm in the pre-, intra- and postoperative phase, and vital signs and reflexes should be checked on a regular basis to confirm the appropriate level of anesthesia. Monitoring equipment (e.g., electrocardiogram, pulse oximeter) should be used for more complicated surgical procedures. When not used, a regular visual assessment of vital signs including color of skin and mucosae and breathing pattern and frequency should be evaluated at regular intervals. Of note, heart rate can only be assessed visually during open thorax surgery. Administering SC fluids at body temperature will prevent dehydration, especially occurring during prolonged procedures. Postoperatively, animals should be recovered in a warm and quiet environment and evaluated frequently until they are sufficiently awake after which they should have easy access to food and water.

age, sex or even individual animals[111–115]. Therefore, it is important to start with a robust literature study and a pilot toxicity study before study commencement. Pilot studies should determine the lowest effective carcinogen dose while limiting adverse effects (e.g., bone marrow suppression or diarrhea in radiation-induced models[116]) and the optimal administration route. Moreover, pilot studies facilitate the assessment of negative effects on animal welfare, carcinogen-related health issues and definition of appropriate endpoints.

Tumor resection models. Surgical resection of primary tumors (grafted or GEM) can be performed in several settings including models of spontaneous metastasis and models of advanced disease in tumors wherein resection is usually the first treatment (e.g., brain[117]). Specifically in the context of metastases, tumor resection assists where HEPs limit the duration of the study either due to tumor size (e.g., breast cancer[118] or osteosarcoma[119]) or clinical condition of the animals in aggressive cancers (e.g., pancreas[120]). While it is beyond the scope of this manuscript to provide details on all such models, the following general steps are recommended. First, perform a pilot study to assess whether recurrence occurs, metastasis develops and survival increases following tumor resection[121]. Second, if resection is necessary to answer the scientific question, assess the optimal time for primary resection to limit welfare impairment as much as possible. It is usually not necessary to wait until the tumor approaches maximum size. Of note tumor resection timepoints differ per organ. Should tumor volume measurements be unavailable, resection upon reaching exponential growth phase, as determined by bioluminescence, is a suitable approach to ensure recurrence[122]. In contrast to surgical implantation of tumors wherein animals are usually healthy, in surgical resection models, animals are tumor bearing and thus by definition not healthy. Peri-operative care should therefore be adapted accordingly.

Humanized mouse models. In general, three different methods are used to reconstitute human immune lineage in immune deficient mice: (1) direct infusion of mature human immune cells, most commonly used source are peripheral blood mononuclear cells, (2) engraftment with human $CD34^+$ hematopoietic stem and progenitor cells upon host preconditioning to deplete endogenous immune cells and (3) co-engraftment of human fetal thymus tissue and liver CD34+ hematopoietic stem and progenitor cells. Depending on the method of humanization, various adverse effects can be expected of which graft-versus-host-disease (GVHD), tumor growth inhibition, efficiency impairment of lymphocytes and anemia are the most common ones[123]. These adverse effects can mostly be prevented by selecting the optimal engraftment strategy and immune deficient mouse for answering the experimental question. For example, a model with delayed GVHD should be used when study duration is longer. Models with rapid onset of GVHD should not be used when study duration is longer (than 4–5 weeks). See also intravenous injection and intra-abdominal implantation for main points of refinement in developing humanized mice.

Clinical consequences of different cancer models

As discussed, adverse effects and clinical consequences for the animal can differ substantially depending on the tumor model. Therefore, animal monitoring procedures, refinement options and HEPs should be adapted accordingly. Table 1 describes which clinical signs or adverse effects may be expected in different tumors regardless of the model (primary versus metastatic, orthotopic implantation versus carcinogen, for example). We decided to distinguish pain into 'demonstrated' when studies have shown that these tumors are painful and 'assumed' when studies specifically aimed at measuring pain are lacking but when these tumor types are known to be painful in human patients. Anorexia/BW loss and altered appearance/behavior are usually not expected in certain tumor types. However, depending on the aggressiveness of the tumor, these characteristics may be observed (Box 4).

In Table 2, the clinical signs or adverse effects are further outlined. We also elaborate on how these signs can be recognized in rodents and why these may occur in a cancer setting. To assess certain clinical signs, specific tests are recommended. While we chose to recommend easy to perform and minimally invasive tests, such as the stress-test for the assessment of labored breathing (Fig. 3), other more invasive tests or tests requiring specific equipment could be used to assess the animal. We therefore acknowledge that these recommendations are not exhaustive.

https://doi.org/10.1038/s41596-024-00998-w

BOX 3

Stepwise approach on using the monitoring sheets and defining HEPs for your model

1. Check Table 1 to see which adverse effects are expected in the model.
2. Check Table 2 to see how to assess these adverse effects.
3. Select the appropriate monitoring sheets based on the expected adverse effects.
4. If surgery is involved, also include the postsurgical monitoring sheet (Table 5).
5. Check Table 3 for follow-up of the tumor.
6. Combine the different monitoring sheets + size/appearance of the tumor to obtain a final monitoring sheet with appropriate HEPs.
   An example of a tailored monitoring sheet can be found in the Supplementary Information.

Refinement during tumor development

Refinement of an ongoing in vivo study should be performed in a two-fold manner. First by adapting the monitoring of the animals to the expected adverse effects (i.e., choice of which signs to monitor and the frequency of the monitoring) and second by taking appropriate action based on adverse effects. It is important to note that monitoring the animals implies monitoring the tumor itself (mainly size and/or appearance) and, in parallel, observing the clinical condition of the animal.

Monitoring of tumors. Depending on the location and type of model, different methods can be employed to determine tumor characteristics (e.g., size). Table 3 provides an overview of tumor assessment over time. We will not discuss in detail the different techniques for tumor assessment, rather we will focus on aspects affecting animal welfare or study outcome and reproducibility. The criteria for animal killing are solely based on tumor aspect and not on the clinical condition of the animal. The latter are described in the other monitoring sheets (Tables 4–12).

BOX 4

Body and tumor weight in cancer studies

How to determine baseline BW?

BW loss (actual weight compared with baseline weight) is often used to determine HEPs. In studies wherein tumors are implanted in adult animals, baseline BW = BW at the start of the study. When animals are implanted at a younger age, BW at study start might not be the correct value to assess weight loss, especially in slow-growing tumors.

Illustrative example: an 18 g mouse is implanted with a slow-growing tumor. During tumor development the animal grows to 25 g. Assume the mouse starts to show adverse effects from then on, including weight loss. Humane killing upon 20% weight loss based on 25 g baseline weight should be done when the animal reaches 20 g. Considering 18 g as baseline BW would imply humane killing at 14.4 g or 42% BW loss.

Therefore, baseline BW in growing animals (especially in slow-growing tumors) should be based on growth curves and/or discussed with the animal welfare officer or facility veterinarian.

BW increase in tumor studies?

Although BW loss often occurs during mouse tumor studies, some models may also cause an increase in BW (e.g., due to ascites or splenomegaly) and can even aid in determining HEPs[29].

Should we consider tumor weight when measuring BW?

Although tumor volume is often measured in studies and we know that 1 cm^3 of tumor weighs 1 g (ref. 126), tumor weight will only remarkably influence weight (>10%, indicated in boldface) in very small mice (<20 g) or in very large tumors (exceeding the criteria for humane killing) in mice. Consider using larger mice in long-term studies or when studying fast-growing tumors. This only applies to mice and not rats since the tumor/BW ratio is very different in rats compared with mice.

The table below shows the percentages of tumor weight as a function of mouse weight.

Tumor		Mouse weight (g)												
Volume	**Weight**	**18**	**19**	**20**	**21**	**22**	**23**	**24**	**25**	**26**	**27**	**28**	**29**	**30**
		Percentage of tumor weight in function of BW												
0.5 cm^3	0.5 g	2.8	2.6	2.5	2.4	2.3	2.2	2.1	2.0	1.9	1.9	1.8	1.7	1.7
1 cm^3	1 g	5.6	5.3	5.0	4.8	4.5	4.3	4.2	4.0	3.8	3.7	3.6	3.4	3.3
1.5 cm^3	1.5 g	8.3	7.9	7.5	7.1	6.8	6.5	6.3	6.0	5.8	5.6	5.4	5.2	5.0
2 cm^3	2 g	**11.1**	**10.5**	**10.0**	9.5	9.1	8.7	8.3	8.0	7.7	7.4	7.1	6.9	6.7
2.5 cm^3	2.5 g	**13.9**	**13.2**	**12.5**	**11.9**	**11.4**	**10.9**	**10.4**	**10.0**	9.6	9.3	8.9	8.6	8.3
3 cm^3	3 g	**16.7**	**15.8**	**15.0**	**14.3**	**13.6**	**13.0**	**12.5**	**12.0**	**11.5**	**11.1**	**10.7**	**10.3**	**10.0**

https://doi.org/10.1038/s41596-024-00998-w

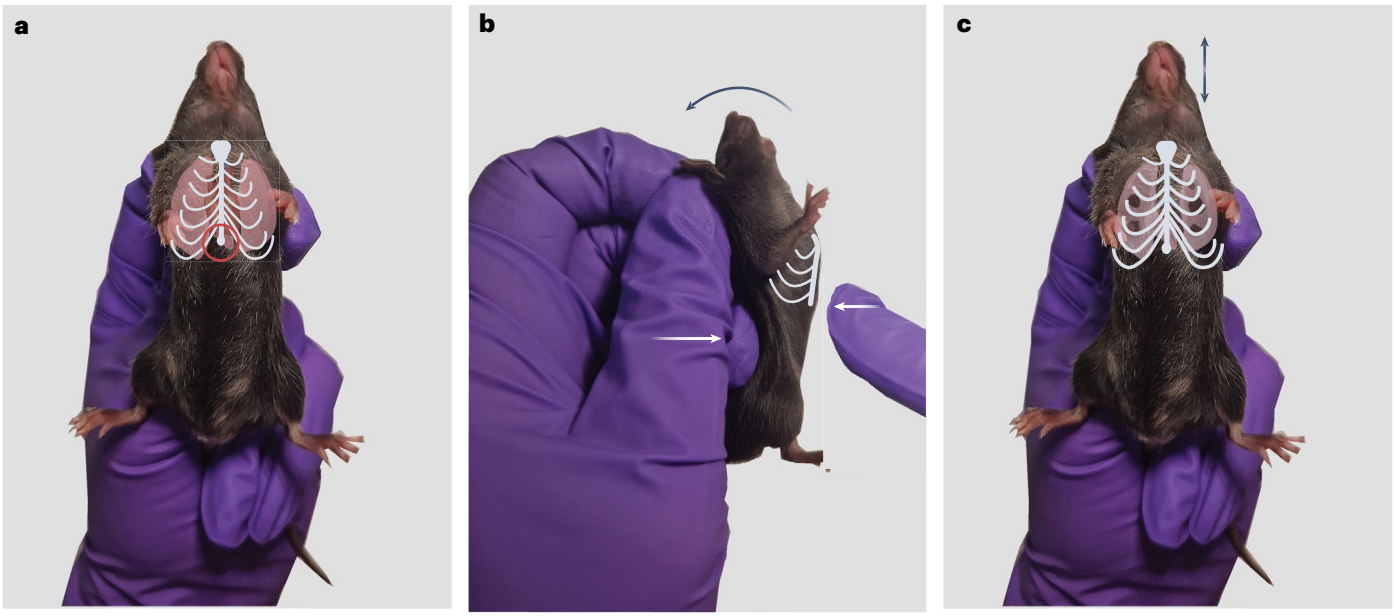

Fig. 3 | Step-by-step description of a stress test. a,**b**, A stress-test should be performed by restraining the mouse as demonstrated in **a** and pressing the xyphoid with the finger of the dominant hand as demonstrated in **b**. Gentle-to-moderate pressure should be applied for 3 s. The red circle in **a** indicates the xyphoid where pressure should be applied. The arrows in **b** and **c** indicate the important features when holding the mice.

Monitoring of animals with different tumor models. As discussed above and listed in Table 2, different tumor types may manifest different adverse effects, mainly depending on their location. Although some adverse effects are general and occur in most models (Table 4), others may greatly differ between different models and are very specific, for example, postoperative care (Table 5). Here, we provide clear guidelines on how to monitor animals throughout the study based on expected adverse effects. As scoresheets imply annotating numerical scores to clinical parameters and often require the calculation of a final score to make an informed decision on the animal's fate; we chose to propose monitoring sheets without numerical scores, which can more easily be combined with a complete monitoring sheet adapted for the varying adverse effects across a variety of tumor models. Monitoring sheets include which parameters to observe, the frequency of monitoring and actions to be taken. In addition, refinement options and criteria for humane methods of killing are described.

Monitoring animals for model-specific adverse effects. For cases in which adverse effects occur predominantly in specific tumor models, we present monitoring sheets that group signs by clinical category. Animals may suffer respiratory difficulties (Table 6), neurological changes (Table 7), locomotor issues (Table 8), GI issues (Table 9) and/or urinary signs (Table 10).

Monitoring animals with tumors causing ascites. Ascites—a condition in which fluid accumulates in the abdomen—is a rare adverse effect, and animals should be culled as soon as possible once this condition develops. When ascites is the main research objective, however, the monitoring sheet in Table 11 may be used.

Correct drainage of ascitic fluid or ascitic taps. When ascitic fluid needs draining, a series of points need to be followed:

- The mouse needs to be manually restrained, held in a vertical position with the head pointing upward. Inexperienced personnel may anesthetize the mice by using isoflurane
- The abdominal surface needs to be shaved and disinfected before the insertion of the needle
- The size of the sterile needle should be the smallest possible (25–22G) to allow good flow. Needle insertion should be in the lower left or right quadrant of the abdomen
- The ascites fluid needs to be allowed to drip from the needle hub (aspirating fluid may cause circulatory decompression and shock). Rotation of the needle and adjusting the depth of insertion will allow for optimizing the rate of collection. When the ascites is viscous, collection is more efficient if the needle is removed and the fluid is allowed to drip from the puncture. Indicatively, one drop every 3 or 4 s is considered a good flow rate
- When collection is completed, the puncture site needs to be disinfected again before the animal is returned to its cage
- The animal should be observed for 30 min after tap for signs of shock or discomfort

Monitoring animals with cutaneous ulcerating tumors. The ulceration of tumors is usually considered an endpoint (Table 3). However, there are exceptional circumstances where ulcers are tolerated and premature killing is postponed, thereby avoiding the loss of potential important data. Exceptions should be only considered if:

- Models are known to be prone to ulceration
- Late-stage cancer models that often present with ulcerating tumors
- Ulcerated tumors that are healed following therapeutic intervention

Noteworthy, erroneously intradermal instead of SC engraftment could lead to fast necrosis and ulcerative tumors. Appropriate training and proper SC injection could limit ulcer development. In Table 12, the different ulcerative lesions are described, including a score for each type of lesion, the necessary interventions and the mandatory monitoring frequency.

Monitoring animals with tumors causing cachexia. Cachexia is a condition where a tumor (or other chronic illness) causes weakness and wasting of the body. Animals should be killed before they become cachectic unless in models wherein cancer cachexia is the main research objective[124,125]. In all other cancer models, HEPs should be applied to avoid cachexia. Animals in cancer cachexia studies should

be culled no later than having reached 25% BW loss, also taking into account the measurement of tumor volume[126,127].

Monitoring animals with tumors causing icterus. Icterus (jaundice) is a sign of advanced disease, animals should be humanely killed when diagnosed.

Monitoring animals with tumors causing anemia. When anemia is detected on visual assessment of the animal, the animals should be humanely killed as this is a sign of advanced disease.

Severity assessment

According to the EU directive 2010/63/EU, all animal procedures need to be classified as mild, moderate or severe. However, severity assessment of animal procedures and models remains a difficult task and unfortunately few resources exist on how to consistently classify mouse cancer models, in particular orthotopic and complex models with multiple adverse effects are particularly difficult to consistently classify.

Therefore, in Table 13, we propose a severity classification for a variety of cancer models based on clinical signs, tumor characteristics and implantation method. Note that the severity assessment should take into account all of the above and that the HEPs described throughout the guidelines are crucial in this assessment. If endpoints are exceeded, severity must be scored higher than what was proposed prospectively. Importantly, as some models are always accompanied by severe adverse effects, these models are classified as severe by default, e.g., models requiring ascitic tap or cancer pain models.

Conclusions

The OBSERVE guidelines bridge the existing gap between appropriate preparation and reporting of in vivo cancer studies in rodents. By focusing on refinement during animal experiments, researchers and animal care staff are provided with precise and practical guidance on how to implement the optimal preparation and implantation methods. Also, expected adverse effects and clinical signs associated with organ-specific tumor development are clearly described including etiology and guidelines for assessment. In addition, hands-on tools and precise monitoring criteria during tumor development are provided at two levels: how to monitor tumor proliferation and how to follow-up the animal. The latter is done by providing a comprehensive and specific set of monitoring sheets for rodents with a variety of clinical signs, regardless of their origin, and incorporate HEPs that are based on expected adverse effects per tumor type. At last, a robust guidance on severity assessment is provided based on clinical consequences, implantation method and characteristics of the tumor.

Since reliable animal-free alternatives are not yet widely available, in vivo experiments remain an important step in unravelling complex biological questions. Nevertheless, animal experiments that are still required must be performed in the most optimal and ethical way. Therefore, the current refinement guidelines fill an important gap by providing a practical resource for a large number of cancer research laboratories. We strongly believe major improvements can be generated in workflows of in vivo experimentation, thereby minimizing the level of severity in the most common murine models and reducing unnecessary distress and pain. The guidelines can largely contribute to animal welfare and the refinement of animal studies in cancer research.

References

1. O'Brien, S. G. et al. Imatinib compared with interferon and low-dose cytarabine for newly diagnosed chronic-phase chronic myeloid leukemia. *N. Engl. J. Med.* **348**, 994–1004 (2003).
2. Fazio, M., Ablain, J., Chuan, Y., Langenau, D. M. & Zon, L. I. Zebrafish patient avatars in cancer biology and precision cancer therapy. *Nat. Rev. Cancer* **20**, 263–273 (2020).
3. Pauli, C. et al. Personalized in vitro and in vivo cancer models to guide precision medicine. *Cancer Discov.* **7**, 462–477 (2017).
4. Le Magnen, C., Dutta, A. & Abate-Shen, C. Optimizing mouse models for precision cancer prevention. *Nat. Rev. Cancer* **16**, 187––196 (2016).
5. Animals used for scientific purposes. *European Commission* https://ec.europa.eu/environment/chemicals/lab_animals/alures_en.htm (2022).
6. Guillen, K. P. et al. A human breast cancer-derived xenograft and organoid platform for drug discovery and precision oncology. *Nat. Cancer* **3**, 232–250 (2022).
7. Honkala, A., Malhotra, S. V., Kummar, S. & Junttila, M. R. Harnessing the predictive power of preclinical models for oncology drug development. *Nat. Rev. Drug Discov.* **21**, 99–114 (2022).
8. Cuppens, T. et al. Potential targets' analysis reveals dual PI3K/mTOR pathway inhibition as a promising therapeutic strategy for uterine leiomyosarcomas—an ENITEC group initiative. *Clin. Cancer Res.* **23**, 1274–1285 (2017).
9. Hebert, J. D., Neal, J. W. & Winslow, M. M. Dissecting metastasis using preclinical models and methods. *Nat. Rev. Cancer* **23**, 391–407 (2023).
10. Perse, M. Cisplatin mouse models: treatment, toxicity and Translatability. *Biomedicines* **9**, 1406 (2021).
11. Karkampouna, S. et al. Patient-derived xenografts and organoids model therapy response in prostate cancer. *Nat. Commun.* **12**, 1117 (2021).
12. Patton, E. E. et al. Melanoma models for the next generation of therapies. *Cancer Cell* **39**, 610–631 (2021).
13. Zitvogel, L., Pitt, J. M., Daillere, R., Smyth, M. J. & Kroemer, G. Mouse models in oncoimmunology. *Nat. Rev. Cancer* **16**, 759–773 (2016).
14. Gardner, E. E. & Rudin, C. M. Drug therapy: preclinical oncology—reporting transparency needed. *Nat. Rev. Clin. Oncol.* **13**, 8–9 (2016).
15. Amaral, O. B. & Neves, K. Reproducibility: expect less of the scientific paper. *Nature* **597**, 329–331 (2021).
16. Pritt, S. L. & Hammer, R. E. The interplay of ethics, animal welfare, and IACUC oversight on the reproducibility of animal studies. *Comp. Med.* **67**, 101–105 (2017).
17. Cheleuitte-Nieves, C. & Lipman, N. S. Improving replicability, reproducibility, and reliability in preclinical research: a shared responsibility. *ILAR J.* **60**, 113–119 (2019).
18. Errington, T. M. et al. Investigating the replicability of preclinical cancer biology. *eLife* **10**, e.71601 (2021).
19. Smith, A. J., Clutton, R. E., Lilley, E., Hansen, K. E. A. & Brattelid, T. PREPARE: guidelines for planning animal research and testing. *Lab. Anim.* **52**, 135–141 (2018).
20. Kilkenny, C., Browne, W. J., Cuthill, I. C., Emerson, M. & Altman, D. G. Improving bioscience research reporting: the ARRIVE guidelines for reporting animal research. *PLoS Biol.* **8**, e1000412 (2010).
21. Percie du Sert, N. et al. The ARRIVE guidelines 2.0: updated guidelines for reporting animal research. *PloS Biol.* **18**, e3000410 (2020).
22. EU Parliament event on animal research. *European Animal Resarch Association* https://www.eara.eu/post/eu-parliament-event-on-animal-research (2022).
23. Russell, W. M. S. & Burch, R. L. *The Principles of Humane Experimental Technique*. (Methuen, 1959).
24. Tannenbaum, J. & Bennett, B. T. Russell and Burch's 3Rs then and now: the need for clarity in definition and purpose. *J. Am. Assoc. Lab. Anim. Sci.* **54**, 120–132 (2015).
25. Workman, P. et al. Guidelines for the welfare and use of animals in cancer research. *Br. J. Cancer* **102**, 1555–1577 (2010).
26. Wallace, J. Humane endpoints and cancer research. *ILAR J.* **41**, 87–93 (2000).

27. Workman, P. et al. UKCCCR guidelines for the welfare of animals in experimental neoplasia. *Lab. Anim.* **22**, 195–201 (1988).
28. Winn, C. B. et al. Automated monitoring of respiratory rate as a novel humane endpoint: a refinement in mouse metastatic lung cancer models. *PLoS ONE* **16**, e0257694 (2021).
29. Aldred, A. J., Cha, M. C. & Meckling-Gill, K. A. Determination of a humane endpoint in the L1210 model of murine leukemia. *Contemp. Top. Lab. Anim. Sci.* **41**, 24–27 (2002).
30. Paster, E. V., Villines, K. A. & Hickman, D. L. Endpoints for mouse abdominal tumor models: refinement of current criteria. *Comp. Med.* **59**, 234–241 (2009).
31. Helgers, S. O. A. et al. Body weight algorithm predicts humane endpoint in an intracranial rat glioma model. *Sci. Rep.* **10**, 9020 (2020).
32. Oliveira, M. et al. Implementation of humane endpoints in a urinary bladder carcinogenesis study in rats. *Vivo* **31**, 1073–1080 (2017).
33. Silva-Reis, R. et al. Refinement of animal model of colorectal carcinogenesis through the definition of novel humane endpoints. *Animals* **11**, 985 (2021).
34. Akladios, C., Ignat, M., Mutter, D. & Aprahamian, M. Survival variability of controls and definition of imaging endpoints for longitudinal follow-up of pancreatic ductal adenocarcinoma in rats. *J. Cancer Res. Clin. Oncol.* **143**, 29–34 (2017).
35. Kobaek-Larsen, M., Rud, L., Oestergaard Soerensen, F. & Ritskes-Hoitinga, J. Laparoscopy of rats with experimental liver metastases: a method to assess new humane endpoints. *Lab. Anim.* **38**, 162–168 (2004).
36. Percie du Sert, N. et al. The IMPROVE guidelines (ischaemia models: procedural refinements of in vivo experiments). *J. Cereb. Blood Flow. Metab.* **37**, 3488–3517 (2017).
37. Mirzoyan, Z. et al. *Drosophila melanogaster*: a model organism to study cancer. *Front. Genet.* **10**, 51 (2019).
38. Yamamura, R., Ooshio, T. & Sonoshita, M. Tiny *Drosophila* makes giant strides in cancer research. *Cancer Sci.* **112**, 505–514 (2021).
39. Robertson, N., Schook, L. B. & Schachtschneider, K. M. Porcine cancer models: potential tools to enhance cancer drug trials. *Expert Opin. Drug Discov.* **15**, 893–902 (2020).
40. Oh, J. H. & Cho, J. Y. Comparative oncology: overcoming human cancer through companion animal studies. *Exp. Mol. Med.* **55**, 725–734 (2023).
41. Deycmar, S., Gomes, B., Charo, J., Ceppi, M. & Cline, J. M. Spontaneous, naturally occurring cancers in non-human primates as a translational model for cancer immunotherapy. *J. Immunother. Cancer* **11**, e005514 (2023).
42. Cannon, C. M. Cats, cancer and comparative oncology. *Vet. Sci.* **2**, 111–126 (2015).
43. Overgaard, N. H. et al. Of mice, dogs, pigs, and men: choosing the appropriate model for immuno-oncology research. *ILAR J.* **59**, 247–262 (2018).
44. LeBlanc, A. K. & Mazcko, C. N. Improving human cancer therapy through the evaluation of pet dogs. *Nat. Rev. Cancer* **20**, 727–742 (2020).
45. Schook, L. B. et al. A genetic porcine model of cancer. *PLoS ONE* **10**, e0128864 (2015).
46. Kalla, D. et al. The missing link: cre pigs for cancer research. *Front. Oncol.* **11**, 755746 (2021).
47. Kalla, D., Kind, A. & Schnieke, A. Genetically engineered pigs to study cancer. *Int. J. Mol. Sci.* **21**, 488 (2020).
48. Astell, K. R. & Sieger, D. Zebrafish in vivo models of cancer and metastasis. *Cold Spring Harb. Perspect. Med.* **10**, a037077 (2020).
49. Jiang, H., Kimura, T., Hai, H., Yamamura, R. & Sonoshita, M. *Drosophila* as a toolkit to tackle cancer and its metabolism. *Front. Oncol.* **12**, 982751 (2022).
50. Hendricks-Wenger, A. et al. Employing novel porcine models of subcutaneous pancreatic cancer to evaluate oncological therapies. *Methods Mol. Biol.* **2394**, 883–895 (2022).
51. Callesen, M. M. et al. A genetically inducible porcine model of intestinal cancer. *Mol. Oncol.* **11**, 1616–1629 (2017).
52. Boas, F. E. et al. Induction and characterization of pancreatic cancer in a transgenic pig model. *PLoS ONE* **15**, e0239391 (2020).
53. Saur, D. & Schnieke, A. Porcine cancer models for clinical translation. *Nat. Rev. Cancer* **22**, 375–376 (2022).
54. Jarvis, S. et al. Non-rodent animal models of osteosarcoma: a review. *Cancer Treat. Res. Commun.* **27**, 100307 (2021).
55. Penet, M. F. et al. Ascites volumes and the ovarian cancer microenvironment. *Front. Oncol.* **8**, 595 (2018).
56. Sale, S. & Orsulic, S. Models of ovarian cancer metastasis: murine models. *Drug Discov. Today Dis. Models* **3**, 149––154 (2006).
57. Zakarya, R., Howell, V. M. & Colvin, E. K. Modelling epithelial ovarian cancer in mice: classical and emerging approaches. *Int. J. Mol. Sci.* **21**, 4806 (2020).
58. Ehlich, H. et al. INFRAFRONTIER quality principles in systemic phenotyping. *Mamm., Genome* **33**, 120–122 (2022).
59. Meehan, T. F. et al. PDX-MI: minimal information for patient-derived tumor xenograft models. *Cancer Res.* **77**, e62–e66 (2017).
60. Peterson, N. C. From bench to cageside: risk assessment for rodent pathogen contamination of cells and biologics. *ILAR J.* **49**, 310–315 (2008).
61. Nicklas, W., Kraft, V. & Meyer, B. Contamination of transplantable tumors, cell lines, and monoclonal antibodies with rodent viruses. *Lab. Anim. Sci.* **43**, 296–300 (1993).
62. Geraghty, R. J. et al. Guidelines for the use of cell lines in biomedical research. *Br. J. Cancer* **111**, 1021–1046 (2014).
63. Chateau-Joubert, S. et al. Spontaneous mouse lymphoma in patient-derived tumor xenografts: the importance of systematic analysis of xenografted human tumor tissues in preclinical efficacy trials. *Transl. Oncol.* **14**, 101133 (2021).
64. Diehl, K. H. et al. A good practice guide to the administration of substances and removal of blood, including routes and volumes. *J. Appl. Toxicol.* **21**, 15–23 (2001).
65. Turner, P. V., Brabb, T., Pekow, C. & Vasbinder, M. A. Administration of substances to laboratory animals: routes of administration and factors to consider. *J. Am. Assoc. Lab. Anim. Sci.* **50**, 600–613 (2011).
66. Glascock, J. J. et al. Delivery of therapeutic agents through intracerebroventricular (ICV) and intravenous (IV) injection in mice. *J. Vis. Exp.* https://doi.org/10.3791/2968 (2011).
67. Blair-Handon, R., Mueller, K. & Hoogstraten-Miller, S. An alternative method for intrathymic injections in mice. *Lab. Anim.* **39**, 248–252 (2010).
68. Okano, M. et al. Orthotopic implantation achieves better engraftment and faster growth than subcutaneous implantation in breast cancer patient-derived xenografts. *J. Mammary Gland Biol. Neoplasia* **25**, 27–36 (2020).
69. Rashid, O. M. et al. An improved syngeneic orthotopic murine model of human breast cancer progression. *Breast Cancer Res. Treat.* **147**, 501–512 (2014).
70. Zhang, G. L., Zhang, Y., Cao, K. X. & Wang, X. M. Orthotopic injection of breast cancer cells into the mice mammary fat pad. *J. Vis. Exp.* https://doi.org/10.3791/58604 (2019).
71. Byrne, A. T. et al. Interrogating open issues in cancer precision medicine with patient-derived xenografts. *Nat. Rev. Cancer* **17**, 254–268 (2017).
72. Tavera-Mendoza, L. E. & Brown, M. A less invasive method for orthotopic injection of breast cancer cells into the mouse mammary gland. *Lab. Anim.* **51**, 85–88 (2017).

73. Katsuta, E. et al. Modified breast cancer model for preclinical immunotherapy studies. *J. Surg. Res.* **204**, 467–474 (2016).
74. Martinez-Sabadell, A., Ovejero Romero, P., Arribas, J. & Arenas, E. J. Protocol to generate a patient derived xenograft model of acquired resistance to immunotherapy in humanized mice. *STAR Protoc.* **3**, 101712 (2022).
75. Krause, S., Brock, A. & Ingber, D. E. Intraductal injection for localized drug delivery to the mouse mammary gland. *J. Vis. Exp.* https://doi.org/10.3791/50692 (2013).
76. Bu, W. & Li, Y. Intraductal injection of lentivirus vectors for stably introducing genes into rat mammary epithelial cells in vivo. *J. Mammary Gland Biol. Neoplasia* **25**, 389–396 (2020).
77. Barahona, M. J., Rojas, J., Uribe, E. A. & Garcia-Robles, M. A. Tympanic membrane rupture during stereotaxic surgery disturbs the normal feeding behavior in rats. *Front. Behav. Neurosci.* **14**, 591204 (2020).
78. Ferry, B. & Gervasoni, D. Improving stereotaxic neurosurgery techniques and procedures greatly reduces the number of rats used per experimental group—a practice report. *Animals* **11**, 2662 (2021).
79. Irtenkauf, S. M. et al. Optimization of glioblastoma mouse orthotopic xenograft models for translational research. *Comp. Med.* **67**, 300–314 (2017).
80. Onn, A. et al. Development of an orthotopic model to study the biology and therapy of primary human lung cancer in nude mice. *Clin. Cancer Res.* **9**, 5532–5539 (2003).
81. Boehle, A. S., Dohrmann, P., Leuschner, I., Kalthoff, H. & Henne-Bruns, D. An improved orthotopic xenotransplant procedure for human lung cancer in SCID bg mice. *Ann. Thorac. Surg.* **69**, 1010–1015 (2000).
82. Kang, Y. et al. Development of an orthotopic transplantation model in nude mice that simulates the clinical features of human lung cancer. *Cancer Sci.* **97**, 996–1001 (2006).
83. Buckle, T. & van Leeuwen, F. W. Validation of intratracheal instillation of lung tumour cells in mice using single photon emission computed tomography/computed tomography imaging. *Lab. Anim.* **44**, 40–45 (2010).
84. Nakajima, T. et al. Orthotopic lung cancer murine model by nonoperative transbronchial approach. *Ann. Thorac. Surg.* **97**, 1771–1775 (2014).
85. Das, S., MacDonald, K., Chang, H. Y. & Mitzner, W. A simple method of mouse lung intubation. *J. Vis. Exp.* **73**, e50318 (2013).
86. Brown, R. H., Walters, D. M., Greenberg, R. S. & Mitzner, W. A method of endotracheal intubation and pulmonary functional assessment for repeated studies in mice. *J. Appl. Physiol.* **87**, 2362–2365 (1999).
87. Roughan, J. V., Bertrand, H. G. & Isles, H. M. Meloxicam prevents COX-2-mediated post-surgical inflammation but not pain following laparotomy in mice. *Eur. J. Pain.* **20**, 231–240 (2016).
88. Kashtan, H. et al. Intra-rectal injection of tumour cells: a novel animal model of rectal cancer. *Surg. Oncol.* **1**, 251–256 (1992).
89. Richon, S., Zajac, O., Perez Gonzalez, C. & Matic Vignjevic, D. Optimized protocol for the generation of an orthotopic colon cancer mouse model and metastasis. *STAR Protoc.* **4**, 102022 (2023).
90. Zigmond, E. et al. Utilization of murine colonoscopy for orthotopic implantation of colorectal cancer. *PLoS ONE* **6**, e28858 (2011).
91. Hite, N. et al. An optimal orthotopic mouse model for human colorectal cancer primary tumor growth and spontaneous metastasis. *Dis. Colon Rectum* **61**, 698–705 (2018).
92. McVeigh, L. E. et al. Development of orthotopic tumour models using ultrasound-guided intrahepatic injection. *Sci. Rep.* **9**, 9904 (2019).
93. Huynh, A. S. et al. Development of an orthotopic human pancreatic cancer xenograft model using ultrasound guided injection of cells. *PLoS ONE* **6**, e20330 (2011).
94. Camara Serrano, J. A. Ultrasound guided surgery as a refinement tool in oncology research. *Animals* **12**, 3445 (2022).
95. RA, V. A. N. N. et al. Tissue-directed implantation using ultrasound visualization for development of biologically relevant metastatic tumor xenografts. *Vivo* **31**, 779–791 (2017).
96. Jager, W. et al. Ultrasound-guided intramural inoculation of orthotopic bladder cancer xenografts: a novel high-precision approach. *PLoS ONE* **8**, e59536 (2013).
97. Hadaschik, B. A. et al. A validated mouse model for orthotopic bladder cancer using transurethral tumour inoculation and bioluminescence imaging. *BJU Int.* **100**, 1377–1384 (2007).
98. Watanabe, T. et al. An improved intravesical model using human bladder cancer cell lines to optimize gene and other therapies. *Cancer Gene Ther.* **7**, 1575–1580 (2000).
99. Yardeni, T., Eckhaus, M., Morris, H. D., Huizing, M. & Hoogstraten-Miller, S. Retro-orbital injections in mice. *Lab. Anim.* **40**, 155–160 (2011).
100. Leon-Rico, D. et al. Comparison of haematopoietic stem cell engraftment through the retro-orbital venous sinus and the lateral vein: alternative routes for bone marrow transplantation in mice. *Lab. Anim.* **49**, 132–141 (2015).
101. Li, Q. et al. Analyses of very early hemopoietic regeneration after bone marrow transplantation: comparison of intravenous and intrabone marrow routes. *Stem Cells* **25**, 1186–1194 (2007).
102. Kushida, T. et al. Intra-bone marrow injection of allogeneic bone marrow cells: a powerful new strategy for treatment of intractable autoimmune diseases in MRL/lpr mice. *Blood* **97**, 3292–3299 (2001).
103. Sawyer, G. J. et al. Cardiovascular function following acute volume overload for hydrodynamic gene delivery to the liver. *Gene Ther.* **14**, 1208–1217 (2007).
104. Suda, T., Gao, X., Stolz, D. B. & Liu, D. Structural impact of hydrodynamic injection on mouse liver. *Gene Ther.* **14**, 129–137 (2007).
105. Campbell, J. P., Merkel, A. R., Masood-Campbell, S. K., Elefteriou, F. & Sterling, J. A. Models of bone metastasis. *J. Vis. Exp.* **4**, e4260 (2012).
106. Zhou, H. & Zhao, D. Ultrasound imaging-guided intracardiac injection to develop a mouse model of breast cancer brain metastases followed by longitudinal MRI. *J. Vis. Exp.* https://doi.org/10.3791/51146 (2014).
107. Stocking, K. L. et al. Use of low-molecular-weight heparin to decrease mortality in mice after intracardiac injection of tumor cells. *Comp. Med.* **59**, 37–45 (2009).
108. Gehling, A. M. et al. evaluation of volume of intramuscular injection into the caudal thigh muscles of female and male BALB/c mice (*Mus musculus*). *J. Am. Assoc. Lab. Anim. Sci.* **57**, 35–43 (2018).
109. Pfeiffenberger, U. et al. Assessment and refinement of intra-bone marrow transplantation in mice. *Lab. Anim.* **49**, 121–131 (2015).
110. Uluckan, O., Segaliny, A., Botter, S., Santiago, J. M. & Mutsaers, A. J. Preclinical mouse models of osteosarcoma. *Bonekey Rep.* **4**, 670 (2015).
111. Abel, E. L., Angel, J. M., Kiguchi, K. & DiGiovanni, J. Multi-stage chemical carcinogenesis in mouse skin: fundamentals and applications. *Nat. Protoc.* **4**, 1350–1362 (2009).
112. Tolba, R., Kraus, T., Liedtke, C., Schwarz, M. & Weiskirchen, R. Diethylnitrosamine (DEN)-induced carcinogenic liver injury in mice. *Lab. Anim.* **49**, 59–69 (2015).
113. Zeng, L., Li, W. & Chen, C. S. Breast cancer animal models and applications. *Zool. Res.* **41**, 477–494 (2020).
114. Rivina, L., Davoren, M. J. & Schiestl, R. H. Mouse models for radiation-induced cancers. *Mutagenesis* **31**, 491–509 (2016).
115. Scholten, D., Trebicka, J., Liedtke, C. & Weiskirchen, R. The carbon tetrachloride model in mice. *Lab. Anim.* **49**, 4–11 (2015).

116. Duran-Struuck, R. & Dysko, R. C. Principles of bone marrow transplantation (BMT): providing optimal veterinary and husbandry care to irradiated mice in BMT studies. *J. Am. Assoc. Lab. Anim. Sci.* **48**, 11–22 (2009).
117. Tang, B., Foss, K., Lichtor, T., Phillips, H. & Roy, E. Resection of orthotopic murine brain glioma. *Neuroimmunol. Neuroinflamm.* **8**, 64–69 (2021).
118. Gast, C. E., Shaw, A. K., Wong, M. H. & Coussens, L. M. Surgical procedures and methodology for a preclinical murine model of de novo mammary cancer metastasis. *J. Vis. Exp.* https://doi.org/10.3791/54852 (2017).
119. Ren, L., Huang, S., Beck, J. & LeBlanc, A. K. Impact of limb amputation and cisplatin chemotherapy on metastatic progression in mouse models of osteosarcoma. *Sci. Rep.* **11**, 24435 (2021).
120. Mallya, K., Gautam, S. K., Aithal, A., Batra, S. K. & Jain, M. Modeling pancreatic cancer in mice for experimental therapeutics. *Biochim. Biophys. Acta Rev. Cancer* **1876**, 188554 (2021).
121. Linxweiler, J. et al. Primary tumor resection decelerates disease progression in an orthotopic mouse model of metastatic prostate cancer. *Cancers* **14**, 737 (2022).
122. Sweeney, K. J. et al. Validation of an imageable surgical resection animal model of glioblastoma (GBM). *J. Neurosci. Methods* **233**, 99–104 (2014).
123. Chuprin, J. et al. Humanized mouse models for immuno-oncology research. *Nat. Rev. Clin. Oncol.* **20**, 192–206 (2023).
124. Deboer, M. D. Animal models of anorexia and cachexia. *Expert Opin. Drug Discov.* **4**, 1145–1155 (2009).
125. Bennani-Baiti, N. & Walsh, D. Animal models of the cancer anorexia–cachexia syndrome. *Support Care Cancer* **19**, 1451–1463 (2011).
126. Euhus, D. M., Hudd, C., LaRegina, M. C. & Johnson, F. E. Tumor measurement in the nude mouse. *J. Surg. Oncol.* **31**, 229–234 (1986).
127. Tomayko, M. M. & Reynolds, C. P. Determination of subcutaneous tumor size in athymic (nude) mice. *Cancer Chemother. Pharmacol.* **24**, 148–154 (1989).
128. Ishida, K. et al. Current mouse models of oral squamous cell carcinoma: genetic and chemically induced models. *Oral. Oncol.* **73**, 16–20 (2017).
129. Naik, K. et al. The histopathology of oral cancer pain in a mouse model and a human cohort. *J. Dent. Res.* **100**, 194–200 (2021).
130. Pacharinsak, C. & Beitz, A. Animal models of cancer pain. *Comp. Med.* **58**, 220–233 (2008).
131. Pineda-Farias, J. B., Saloman, J. L. & Scheff, N. N. Animal models of cancer-related pain: current perspectives in translation. *Front. Pharmacol.* **11**, 610894 (2020).
132. Tetreault, M. P. Esophageal cancer: insights from mouse models. *Cancer Growth Metastasis* **8**, 37–46 (2015).
133. Cardesa, A., Ovelar, M. Y. & Pera, M. in *Digestive System* (eds Carlyle Jones, T., Popp, J. A. & Mohr, U.) 318–322 (Springer Berlin, 1997).
134. Hu, H. et al. Real-time bioluminescence and tomographic imaging of gastric cancer in a novel orthotopic mouse model. *Oncol. Rep.* **27**, 1937–1943 (2012).
135. Hayakawa, Y. et al. Mouse models of gastric cancer. *Cancers* **5**, 92–130 (2013).
136. Bhargava, S., Hotz, B., Buhr, H. J. & Hotz, H. G. An orthotopic nude mouse model for preclinical research of gastric cardia cancer. *Int. J. Colorectal Dis.* **24**, 31–39 (2009).
137. Liu, S. et al. Dynamic observation of the progression of chronic gastritis to gastric cancer in a disease–TCM pattern rat model. *J. Trad. Chin. Med. Sci.* **8**, 124–134 (2021).
138. Herreros-Villanueva, M., Hijona, E., Cosme, A. & Bujanda, L. Mouse models of pancreatic cancer. *World J. Gastroenterol.* **18**, 1286–1294 (2012).
139. Lwin, T. M. et al. Fluorescent humanized anti-CEA antibody specifically labels metastatic pancreatic cancer in a patient-derived orthotopic xenograft (PDOX) mouse model. *Oncotarget* **9**, 37333–37342 (2018).
140. Becker, C. et al. In vivo imaging of colitis and colon cancer development in mice using high resolution chromoendoscopy. *Gut* **54**, 950–954 (2005).
141. Hasty, P. et al. eRapa restores a normal life span in a FAP mouse model. *Cancer Prev. Res.* **7**, 169–178 (2014).
142. Chartier, L. C., Hebart, M. L., Howarth, G. S., Whittaker, A. L. & Mashtoub, S. Affective state determination in a mouse model of colitis-associated colorectal cancer. *PLoS ONE* **15**, e0228413 (2020).
143. Ikenoue, T. et al. A novel mouse model of intrahepatic cholangiocarcinoma induced by liver-specific Kras activation and Pten deletion. *Sci. Rep.* **6**, 23899 (2016).
144. Vogt, A. et al. Alpha-fetoprotein- and CD40 ligand-expressing dendritic cells for immunotherapy of hepatocellular carcinoma. *Cancers* **13**, 3375 (2021).
145. Chen, Z., Li, S., Han, L. & He, X. Optimized protocol for an inducible rat model of liver tumor with chronic hepatocellular injury, inflammation, fibrosis, and cirrhosis. *STAR Protoc.* **2**, 100353 (2021).
146. Odashima, S. Comparative studies on the transplantability of liver cancers induced in rats fed with 3′-methyl-4-dimethylaminoazobenzene for 3–6 months. *Gan* **53**, 325–348 (1962).
147. Pretto, F. et al. Sunitinib prevents cachexia and prolongs survival of mice bearing renal cancer by restraining STAT3 and MuRF-1 activation in muscle. *Oncotarget* **6**, 3043–3054 (2015).
148. Roughan, J. V., Coulter, C. A., Flecknell, P. A., Thomas, H. D. & Sufka, K. J. The conditioned place preference test for assessing welfare consequences and potential refinements in a mouse bladder cancer model. *PLoS ONE* **9**, e103362 (2014).
149. Naito, T., Higuchi, T., Shimada, Y. & Kakinuma, C. An improved mouse orthotopic bladder cancer model exhibiting progression and treatment response characteristics of human recurrent bladder cancer. *Oncol. Lett.* **19**, 833–839 (2020).
150. Philyppov, I. B. et al. Alterations in detrusor contractility in rat model of bladder cancer. *Sci. Rep.* **10**, 19651 (2020).
151. Xiao, Z. et al. Characterization of a novel transplantable orthotopic rat bladder transitional cell tumour model. *Br. J. Cancer* **81**, 638––646 (1999).
152. Ding, J. et al. Current animal models of bladder cancer: awareness of translatability (review). *Exp. Ther. Med.* **8**, 691–699 (2014).
153. Senapati, S. et al. Overexpression of macrophage inhibitory cytokine-1 induces metastasis of human prostate cancer cells through the FAK–RhoA signaling pathway. *Oncogene* **29**, 1293–1302 (2010).
154. Pang, K. et al. Monitoring circulating prostate cancer cells by in vivo flow cytometry assesses androgen deprivation therapy on metastasis. *Cytom. A* **93**, 517–524 (2018).
155. De Ciantis, P. D., Yashpal, K., Henry, J. & Singh, G. Characterization of a rat model of metastatic prostate cancer bone pain. *J. Pain. Res.* **3**, 213–221 (2010).
156. Bosland, M. C., Schlicht, M. J., Horton, L. & McCormick, D. L. The MNU plus testosterone rat model of prostate carcinogenesis. *Toxicol. Pathol.* **50**, 478–496 (2022).
157. Haldorsen, I. S. et al. Multimodal imaging of orthotopic mouse model of endometrial carcinoma. *PLoS ONE* **10**, e0135220 (2015).
158. Baert, T. et al. The dark side of ID8-Luc2: pitfalls for luciferase tagged murine models for ovarian cancer. *J. Immunother. Cancer* **3**, 57 (2015).

159. Rose, G. S. et al. Development and characterization of a clinically useful animal model of epithelial ovarian cancer in the Fischer 344 rat. *Am. J. Obstet. Gynecol.* **175**, 593–599 (1996).
160. He, C. et al. A human papillomavirus-independent cervical cancer animal model reveals unconventional mechanisms of cervical carcinogenesis. *Cell Rep.* **26**, 2636–2650 e2635 (2019).
161. Henkle, T. R. et al. Development of a novel mouse model of spontaneous high-risk hpve6/e7-expressing carcinoma in the cervicovaginal tract. *Cancer Res.* **81**, 4560–4569 (2021).
162. Hamada, K., Ueda, N., Ito, M., Roth, J. A. & Follen, M. The nude rat as an orthotopic model for cervical cancer. *Gynecol. Oncol.* **99**, S159–S165 (2005).
163. Koutcher, J. A. et al. MRI of mouse models for gliomas shows similarities to humans and can be used to identify mice for preclinical trials. *Neoplasia* **4**, 480–485 (2002).
164. Bouckaert, C. et al. Development of a rat model for glioma-related epilepsy. *Int. J. Mol. Sci.* **21**, 6999 (2020).
165. Nagarajan, P. P. et al. Lentiviral-induced spinal cord gliomas in rat model. *Int. J. Mol. Sci.* **22**, 12943 (2021).
166. Shimoyama, M., Tanaka, K., Hasue, F. & Shimoyama, N. A mouse model of neuropathic cancer pain. *Pain* **99**, 167–174 (2002).
167. Mao-Ying, Q.-L. et al. A rat model of bone cancer pain induced by intra-tibia inoculation of Walker 256 mammary gland carcinoma cells. *Biochem. Biophys. Res. Commun.* **345**, 1292–1298 (2006).
168. Yang, H. et al. Proteomic analysis of spinal cord tissue in a rat model of cancer-induced bone pain. *Front. Mol. Neurosci.* **15**, 1009615 (2022).
169. Gelbard, A. et al. An orthotopic murine model of sinonasal malignancy. *Clin. Cancer Res.* **14**, 7348–7357 (2008).
170. Feron, V. J., Woutersen, R. A., van Garderen-Hoetmer, A. & Dreef-van der Meulen, H. C. Upper respiratory tract tumors in Cpb:WU (Wistar random) rats. *Environ. Health Perspect.* **85**, 305–315 (1990).
171. Miller, A. L. & Roughan, J. V. Welfare assessment, end-point refinement and the effects of non-aversive handling in C57BL/6 mice with Lewis lung cancer. *Animals* https://doi.org/10.3390/ani12010023 (2021).
172. Mendoza, A. et al. A novel noninvasive method for evaluating experimental lung metastasis in mice. *J. Am. Assoc. Lab. Anim. Sci.* **52**, 584–589 (2013).
173. Byhardt, R. W., Almagro, U. A., Fish, B. L. & Moulder, J. E. Development of a rat lung cancer model. *Int. J. Radiat. Oncol. Biol. Phys.* **10**, 2125–2130 (1984).
174. Zhu, X. C. et al. Analgesic effects of lappaconitine in leukemia bone pain in a mouse model. *PeerJ* **3**, e936 (2015).
175. Helseth, A., Siegal, G. P., Haug, E. & Bautch, V. L. Transgenic mice that develop pituitary tumors. a model for Cushing's disease. *Am. J. Pathol.* **140**, 1071–1080 (1992).
176. Chang-Wei, H., Li, Y. B., Han, X. Y., Yin, G. F. & Wang, X. R. To explore the change of motor cognitive function in pituitary tumor rats after operation. *Comput. Assist. Surg.* **28**, 2198099 (2023).
177. Kim, W. G., Park, J. W., Willingham, M. C. & Cheng, S. Y. Diet-induced obesity increases tumor growth and promotes anaplastic change in thyroid cancer in a mouse model. *Endocrinology* **154**, 2936–2947 (2013).
178. Snarskaya, E. S., Pylev, L. N., Akhunzyanov, A. A. & Kuznetcova, E. V. Experimental basosquamous carcinoma model in rats. *BioNanoScience* **7**, 423–427 (2017).
179. Stribbling, S. M. & Ryan, A. J. The cell-line-derived subcutaneous tumor model in preclinical cancer research. *Nat. Protoc.* **17**, 2108–2128 (2022).
180. Ehx, G. et al. Xenogeneic graft-versus-host disease in humanized NSG and NSG-HLA-A2/HHD mice. *Front. Immunol.* **9**, 1943 (2018).
181. Lai, H. Y., Chou, T. Y., Tzeng, C. H. & Lee, O. K. Cytokine profiles in various graft-versus-host disease target organs following hematopoietic stem cell transplantation. *Cell Transplant.* **21**, 2033–2045 (2012).
182. Ullman-Cullere, M. H. & Foltz, C. J. Body condition scoring: a rapid and accurate method for assessing health status in mice. *Lab. Anim. Sci.* **49**, 319–323 (1999).
183. Hickman, D. L. & Swan, M. Use of a body condition score technique to assess health status in a rat model of polycystic kidney disease. *J. Am. Assoc. Lab. Anim. Sci.* **49**, 155–159 (2010).
184. Burkholder, T., Foltz, C., Karlsson, E., Linton, C. G. & Smith, J. M. Health evaluation of experimental laboratory mice. *Curr. Protoc. Mouse Biol.* **2**, 145–165 (2012).
185. Raja, S. N. et al. The revised International Association for the Study of Pain definition of pain: concepts, challenges, and compromises. *Pain* **161**, 1976–1982 (2020).
186. Langford, D. J. et al. Coding of facial expressions of pain in the laboratory mouse. *Nat. Methods* **7**, 447–449 (2010).
187. Sotocinal, S. G. et al. The Rat Grimace scale: a partially automated method for quantifying pain in the laboratory rat via facial expressions. *Mol. Pain.* **7**, 55 (2011).
188. Jirkof, P. et al. Assessment of postsurgical distress and pain in laboratory mice by nest complexity scoring. *Lab. Anim.* **47**, 153–161 (2013).
189. Jirkof, P. et al. Burrowing behavior as an indicator of post-laparotomy pain in mice. *Front. Behav. Neurosci.* **4**, 165 (2010).
190. Turner, P. V., Pang, D. S. & Lofgren, J. L. A review of pain assessment methods in laboratory rodents. *Comp. Med.* **69**, 451–467 (2019).
191. Deuis, J. R., Dvorakova, L. S. & Vetter, I. Methods used to evaluate pain behaviors in rodents. *Front. Mol. Neurosci.* **10**, 284 (2017).
192. Wright-Williams, S. L., Courade, J. P., Richardson, C. A., Roughan, J. V. & Flecknell, P. A. Effects of vasectomy surgery and meloxicam treatment on faecal corticosterone levels and behaviour in two strains of laboratory mouse. *Pain* **130**, 108–118 (2007).
193. Do, J. P. et al. Automated and continuous monitoring of animal welfare through digital alerting. *Comp. Med.* **70**, 313–327 (2020).
194. Collins, D. E., Mulka, K. R., Hoenerhoff, M. J., Taichman, R. S. & Villano, J. S. Clinical assessment of urinary tract damage during sustained-release estrogen supplementation in mice. *Comp. Med.* **67**, 11–21 (2017).
195. Pearse, G., Frith, J., Randall, K. J. & Klinowska, T. Urinary retention and cystitis associated with subcutaneous estradiol pellets in female nude mice. *Toxicol. Pathol.* **37**, 227–234 (2009).
196. Guyenet, S. J. et al. A simple composite phenotype scoring system for evaluating mouse models of cerebellar ataxia. *J. Vis. Exp.* https://doi.org/10.3791/1787 (2010).
197. Gao, X. et al. in *Brain Tumors* Vol. 158 (ed. Seano, G.) 199–220 (Springer, 2021).
198. Kelp, A. et al. A novel transgenic rat model for spinocerebellar ataxia type 17 recapitulates neuropathological changes and supplies in vivo imaging biomarkers. *J. Neurosci.* **33**, 9068–9081 (2013).
199. Bieler, L. et al. Motor deficits following dorsal corticospinal tract transection in rats: voluntary versus skilled locomotion readouts. *Heliyon* **4**, e00540 (2018).
200. Brough, D. W., Murkin, J. T., Amos, H. E., Smith, A. I. & Turley, K. D. Comparing variability in measurement of subcutaneous tumors in mice using 3D thermal imaging and calipers. *Comp. Med.* **72**, 364–375 (2022).
201. Jensen, M. M., Jorgensen, J. T., Binderup, T. & Kjaer, A. Tumor volume in subcutaneous mouse xenografts measured by microCT is more accurate and reproducible than determined by 18F-FDG–microPET or external caliper. *BMC Med. Imaging* **8**, 16 (2008).

202. Czerninski, R., Amornphimoltham, P., Patel, V., Molinolo, A. A. & Gutkind, J. S. Targeting mammalian target of rapamycin by rapamycin prevents tumor progression in an oral-specific chemical carcinogenesis model. *Cancer Prev. Res.* **2**, 27–36 (2009).
203. Tanaka, T., Kojima, T., Okumura, A., Yoshimi, N. & Mori, H. Alterations of the nucleolar organizer regions during 4-nitroquinoline 1-oxide-induced tongue carcinogenesis in rats. *Carcinogenesis* **12**, 329–333 (1991).
204. Goetze, R. G. et al. Utilizing high resolution ultrasound to monitor tumor onset and growth in genetically engineered pancreatic cancer models. *J. Vis. Exp.* https://doi.org/10.3791/56979 (2018).
205. Glaser, G. et al. Conventional chemotherapy and oncogenic pathway targeting in ovarian carcinosarcoma using a patient-derived tumorgraft. *PLoS ONE* **10**, e0126867 (2015).
206. Vitetta, E. S. et al. Tumor dormancy and cell signaling. V. Regrowth of the BCL1 tumor after dormancy is established. *Blood* **89**, 4425–4436 (1997).
207. Bruckner, M. et al. Murine endoscopy for in vivo multimodal imaging of carcinogenesis and assessment of intestinal wound healing and inflammation. *J. Vis. Exp.* https://doi.org/10.3791/51875 (2014).
208. Kodani, T. et al. Flexible colonoscopy in mice to evaluate the severity of colitis and colorectal tumors using a validated endoscopic scoring system. *J. Vis. Exp.* **80**, e50843 (2013).
209. Habibollahi, P. et al. Optical Imaging with a cathepsin B activated probe for the enhanced detection of esophageal adenocarcinoma by dual channel fluorescent upper GI endoscopy. *Theranostics* **2**, 227–234 (2012).
210. Dassie, E. et al. Detection of fluorescent organic nanoparticles by confocal laser endomicroscopy in a rat model of Barrett's esophageal adenocarcinoma. *Int. J. Nanomed.* **10**, 6811–6823 (2015).
211. Wong, G. S. et al. Optical imaging of periostin enables early endoscopic detection and characterization of esophageal cancer in mice. *Gastroenterology* **144**, 294–297 (2013).
212. El-Masry, O. S. et al. Oral intragastric DMBA administration induces acute lymphocytic leukemia and other tumors in male Wistar rats. *J. Exp. Pharmacol.* **14**, 87–96 (2022).
213. Tannous, B. A. Gaussia luciferase reporter assay for monitoring biological processes in culture and in vivo. *Nat. Protoc.* **4**, 582–591 (2009).
214. Delgado-SanMartin, J. et al. An innovative non-invasive technique for subcutaneous tumour measurements. *PLoS ONE* **14**, e0216690 (2019).
215. Klerk, C. P. et al. Validity of bioluminescence measurements for noninvasive in vivo imaging of tumor load in small animals. *Biotechniques* **43**, 7–13, 30 (2007).
216. Miller, I. S. et al. Durability of cell line xenograft resection models to interrogate tumor micro-environment targeting agents. *Sci. Rep.* **9**, 9204 (2019).
217. Jarzabek, M. A. et al. Molecular imaging in the development of a novel treatment paradigm for glioblastoma (GBM): an integrated multidisciplinary commentary. *Drug Discov. Today* **18**, 1052–1066 (2013).
218. Zeamari, S., Rumping, G., Floot, B., Lyons, S. & Stewart, F. A. In vivo bioluminescence imaging of locally disseminated colon carcinoma in rats. *Br. J. Cancer* **90**, 1259–1264 (2004).
219. Netufo, O. et al. Refining glioblastoma surgery through the use of intra-operative fluorescence imaging agents. *Pharmaceuticals* **15**, 550 (2022).
220. Christensen, J., Vonwil, D. & Shastri, V. P. Non-invasive in vivo imaging and quantification of tumor growth and metastasis in rats using cells expressing far-red fluorescence protein. *PLoS ONE* **10**, e0132725 (2015).
221. Yang, N. et al. A novel GFP nude rat model to investigate tumor-stroma interactions. *Cancer Cell Int.* **14**, 541 (2014).
222. Hoffman, R. M. Application of GFP imaging in cancer. *Lab. Invest.* **95**, 432–452 (2015).
223. Marien, E., Hillen, A., Vanderhoydonc, F., Swinnen, J. V. & Vande Velde, G. Longitudinal microcomputed tomography-derived biomarkers for lung metastasis detection in a syngeneic mouse model: added value to bioluminescence imaging. *Lab. Invest.* **97**, 24–33 (2017).
224. Nota, T. et al. Safety and feasibility of contrast-enhanced computed tomography with a nanoparticle contrast agent for evaluation of diethylnitrosamine-induced liver tumors in a rat model. *Acad. Radiol.* **30**, 30–39 (2023).
225. Olson, J. D. et al. A gated-7T MRI technique for tracking lung tumor development and progression in mice after exposure to low doses of ionizing radiation. *Radiat. Res.* **178**, 321–327 (2012).
226. Baier, J. et al. Influence of MRI examinations on animal welfare and study results. *Invest. Radiol.* **55**, 507–514 (2020).
227. Song, H. T. et al. Rat model of metastatic breast cancer monitored by MRI at 3 tesla and bioluminescence imaging with histological correlation. *J. Transl. Med.* **7**, 88 (2009).
228. Gui, Q. et al. A new rat model of bone cancer pain produced by rat breast cancer cells implantation of the shaft of femur at the third trochanter level. *Cancer Biol. Ther.* **14**, 193–199 (2013).
229. Ayers, G. D. et al. Volume of preclinical xenograft tumors is more accurately assessed by ultrasound imaging than manual caliper measurements. *J. Ultrasound Med.* **29**, 891–901 (2010).
230. Ghaddar, N. et al. Detection of lung tumor progression in mice by ultrasound imaging. *J. Vis. Exp.* https://doi.org/10.3791/60565 (2020).
231. Chen, J. Y. et al. Application of high-frequency ultrasound for the detection of surgical anatomy in the rodent abdomen. *Vet. J.* **191**, 246–252 (2012).
232. O'Farrell, A. C. et al. Implementing systems modelling and molecular imaging to predict the efficacy of BCL-2 inhibition in colorectal cancer patient-derived xenograft models. *Cancers* **12**, 2978 (2020).
233. Sun, R. et al. A radiomics approach to assess tumour-infiltrating CD8 cells and response to anti-PD-1 or anti-PD-L1 immunotherapy: an imaging biomarker, retrospective multicohort study. *Lancet Oncol.* **19**, 1180–1191 (2018).
234. Aubry, K. et al. FDG-PET/CT of head and neck squamous cell carcinoma in a rat model. *Mol. Imaging Biol.* **11**, 88–93 (2009).
235. Lofgren, J. et al. Analgesics promote welfare and sustain tumour growth in orthotopic 4T1 and B16 mouse cancer models. *Lab. Anim.* **52**, 351–364 (2018).
236. Husmann, K. et al. Primary tumour growth in an orthotopic osteosarcoma mouse model is not influenced by analgesic treatment with buprenorphine and meloxicam. *Lab. Anim.* **49**, 284–293 (2015).
237. Taylor, D. K. Influence of pain and analgesia on cancer research studies. *Comp. Med.* **69**, 501–509 (2019).
238. Strohal, R. et al. Wound management with enzyme alginogels: expert consensus. *Hautarzt* **68**, 36–42 (2017).
239. Chaudhary, A., Bag, S., Banerjee, P. & Chatterjee, J. Wound healing efficacy of Jamun honey in diabetic mice model through reepithelialization, collagen deposition and angiogenesis. *J. Tradit. Complement. Med.* **10**, 529–543 (2020).
240. Mitchell, C. M., Salyards, G. W., Theriault, B. R., Langan, G. P. & Luchins, K. R. Evaluation of pain and distress and therapeutic interventions for rectal prolapse in mice to reduce early study removal. *J. Am. Assoc. Lab. Anim. Sci.* **60**, 692–699 (2021).

241. Levin-Allerhand, J. A., Sokol, K. & Smith, J. D. Safe and effective method for chronic 17beta-estradiol administration to mice. *Contemp. Top. Lab. Anim. Sci.* **42**, 33–35 (2003).
242. Fish, R., Danneman, P. J., Brown, M. & Karas, A. *Anesthesia and Analgesia in Laboratory Animals* (Academic Press, 2011).
243. Flecknell, P. *Laboratory Animal Anaesthesia* (Academic Press, 2015).
244. Foley, P. L., Kendall, L. V. & Turner, P. V. Clinical management of pain in rodents. *Comp. Med.* **69**, 468–489 (2019).

Acknowledgements

K.C. and A.T.B. are funded by a European Union Horizon 2020 research and innovation program, 'COLOSSUS' (grant agreement no. 754923) and 'GLIORESOLVE' (grant agreement no. 101073386), Science Foundation Ireland (grants 18/RI/5759, 20/FFP-P/8884 and 20/FFP-P/8613), Irish Health Research Board (grants ILP-POR-2019-066 and ILP-POR-2022-007), Irish Higher Education Authority and North South Research Program 'RADCOL'. Additional financial support was received from the Beaumont Hospital Foundation.

Author contributions

Conceptualization: S.I.D.V. and E.R.H.; methodology: S.I.D.V., M.v.d.V., K.D., D.R., A.M.R., Y.D.R. and E.R.H.; writing–original draft preparation: S.I.D.V., M.v.d.V., A.O., K.D., K.C., D.R., A.M.R., Y.D.R., M.D., V.D.-M. and E.R.H.; writing–review and editing: S.I.D.V., A.T.B. and E.R.H. All authors have read and agreed to the published version of the manuscript.

Competing interests

The authors declare no competing interests.

Additional information

Supplementary information The online version contains supplementary material available at https://doi.org/10.1038/s41596-024-00998-w.

Correspondence and requests for materials should be addressed to Stéphanie I. De Vleeschauwer.

Peer review information *Nature Protocols* thanks Neil Lipman, Patricia V. Turner and the other, anonymous, reviewer(s) for their contribution to the peer review of this work.

Reprints and permissions information is available at www.nature.com/reprints.

Publisher's note Springer Nature remains neutral with regard to jurisdictional claims in published maps and institutional affiliations.

Stéphanie I. De Vleeschauwer[1] ✉, Marieke van de Ven[2], Anaïs Oudin[3], Karlijn Debusschere[4,10], Kate Connor[5], Annette T. Byrne[5], Doreen Ram[2], Anne Marie Rhebergen[6], Yannick D. Raeves[7], Maik Dahlhoff[8], Virginie Dangles-Marie[9] & Els R. Hermans[2]

[1]Laboratory Animal Center KU Leuven, Leuven, Belgium. [2]Laboratory Animal Facility, The Netherlands Cancer Institute, Amsterdam, the Netherlands. [3]NORLUX Neuro-Oncology Laboratory, Department of Oncology, Luxembourg Institute of Health, Luxembourg, Luxembourg. [4]Animal Core Facility VUB, Brussels, Belgium. [5]Department of Physiology and Medical Physics, Royal College of Surgeons in Ireland, Dublin, Ireland. [6]Genmab, Utrecht, the Netherlands. [7]Janssen Pharmaceutica, Beerse, Belgium. [8]Institute of in vivo and in vitro Models, University of Veterinary Medicine Vienna, Vienna, Austria. [9]In vivo Experiment Platform, PSL Research University, Paris, France. [10]Present address: Core ARTH Animal Facilities, Medicine and Health Sciences Ghent University, Ghent, Belgium.